Understanding the physical, chemical and biological processes across the Subtropical Convergence during austral Autumn.

By

Caren George

Supervised by Dr I.J. Ansorge[1] and Prof P. W. Froneman[2]

[1]*Department of Oceanography, University of Cape Town, Cape Town, South Africa*
[2]*Southern Ocean Group, Department of Zoology and Entomology, Rhodes University, Grahamstown, South Africa*

University of Cape Town
Department of Oceanography

In partial completion of Applied Marine Science Masters 2009

Table of Contents

List of figures and tables

Figures

Tables

Appendices

Acknowledgements

I would like to thank my supervisors, Dr Isabelle Ansorge and Prof William Froneman, for their assistance and advice in all areas of this project, Christo Whittle for his help with the acquisition of the satellite data, Jonathan Durgadoo for data analysis assistance and my family for their continued support. I would like to give many thanks to Coleen Moloney for her comments and suggestions. Thank you to the biological data team from Rhodes University for providing the integrated Chl-a data and the mesozooplankton abundance data, Mr Craig Attwood in the Department of Oceanography for the chemical analysis data and the officers and crew of the S.A. Agulhas. I would also like to thank SANAP for providing funding for this study.

Abstract

A research survey was conducted, consisting of six transects between 38°- 46°S and 38 – 41°45´E, during the austral autumn of 2007. The aim of the survey was to investigate the physical, chemical and biological dynamics of the Subtropical Convergence (STC), in the SW Indian sector of the Southern Ocean. Satellite data was obtained and in-situ data were collected. Mixed layer depth (MLD), geostrophic velocities, density and Brunt Vaisala frequencies were calculated. The STC meandered across the survey area between 41° - 42°15´S. The total integrated Chl-a ranged from 12.8 to 40.1 mg Chl-a/m^2. The most significant correlation between biological and physical data was that of Chl-a and MLD ($r=-0.374$, $n=45$, $p=0.013$) over the entire survey region. Phosphate and nitrate ($r=0.8779$, $n=45$, $p<0.001$) measured over the survey region were strongly correlated, as expected. The surface currents showed cyclonic motion between 38° - 39°E and 38 – 42°S, with the exception of an eddy-like feature between 39.5°and 40.5°S and generally anti-cyclonic motion to the east of 39°E. Satellite imagery showed an intrusion of colder surface water to the north along 39°E and this coincided with an increase in the satellite Chl-a data and a higher observed integrated Chl-a concentration compared to the rest of the survey region. Subtropical, Subantarctic and Mixed water masses were identified and the physical, chemical and biological data were compared. Integrated Chl-a concentration (mean) in Subantarctic water was significantly higher than Subtropical water ($p<0.0001$). Integrated Chl-a concentration (mean) in Mixed water was significantly higher than in Subtropical water ($p=0.02$). The MLD (mean) in Subantarctic water was significantly shallower than in the Subtropical ($p=0.02$) and Mixed water ($p<0.001$). Within the different water masses, the most notable correlation was between nitrate and phosphate concentrations in the Subantarctic water. The evidence suggests that the major factors in controlling Chl-a concentration at the STC are MLD and nutrient availability. These requirements are governed by the water mass mixing across the survey region.

Chapter One - Introduction

Physical Setting of the Southern Ocean

The Southern Ocean is the name given to the oceanic region that surrounds the entire Antarctic continent. It comprises the southern extents of the Atlantic, Indian and Pacific Oceans. The Antarctic continent forms the southern boundary of the Southern Ocean, while the northern border is not physio-graphically fixed, but is usually considered to coincide with the geographic location of the Subtropical Convergence (Lutjeharms 1985). Dominating the flow of the Southern Ocean is the Antarctic Circumpolar Current (ACC) - which, extending unbroken around Antarctica is the primary means by which heat and salt are transferred between different ocean basins. The ACC is the only ocean current that flows around the entire globe and includes a number of different frontal zones (Figure 1). These fronts are regarded as boundaries separating uniform water masses (Lutjeharms, 1985). The Subtropical Convergence (STC), also known as the Subtropical Front (STF), is identified as one of these frontal zones and is considered to be a major front in the global ocean (Lutjeharms et al., 1993).

The Subtropical Convergence

The STC represents the northern boundary to the Southern Ocean. It is the main boundary that separates warm Subtropical waters from cooler, less saline Subantarctic water masses to the south. The geographic position of the front in the different ocean basins is largely determined by the topographical steering of the ACC (Gordon et al., 1978). Additionally, the wind stress curl plays a role in the determination of the frontal positions (Nowlin and Klinck, 1986) through the intensity of the drag created by the wind blowing over the surface. Changes in wind speed or duration consequently affect the intensity of the frontal positions (Trenberth et al., 1990). The position of the STC in the Atlantic and Indian Oceans lies at approximately 40°S (Table 1), which corresponds to

the maximum westerly wind stress curl in the Southern Ocean (Peterson and Stramma, 1991). Although the Subtropical Convergence circles most of the globe, geographically, its intensity varies considerably (Belkin and Gordon, 1996). In the South Atlantic, for instance, it is weak (Smythe-Wright et al., 1998) and ephemeral, consisting of two fronts, the North Subtropical Front (NSTF) and the South Subtropical Front (SSTF), whereas south of Africa between 10°–70°E it is enhanced by the juxtaposition of the warm Agulhas Return Current (Lutjeharms and Ansorge, 2001).

Table 1 Definitions of the mean position of the surface expression of the STC.

Source	Mean Location
Belkin and Gordon (1996)	~38 - 42°S
Lutjeharms and Valentine (1984)	~40°S

Meridional gradients in temperature and/or salinity can be used to describe and assess the intensity of the frontal zones within the ACC (Roden, 1975; Longhurst, 1998). The intensity of these gradients correlates to where the Southern Ocean is in close proximity to the continental masses of the southern hemisphere e.g. Africa (Lutjeharms et al., 1993). Where the fronts occur in the ocean basins, the meridional gradients are much weaker; an example of this would be the observed weaker gradients of the STC across the Atlantic Ocean (Smythe-Wright et al., 1998). The area between 10°E and 70°E exhibits more intense gradients than the other regions of the STC (Lutjeharms and Ansorge, 2001). This intensification of the STC is demonstrated by salinity gradients exceeding 0.06psu/km (Lutjeharms and Ansorge, 2001) and temperature gradients of 0.15°C/km (Lutjeharms and Valentine, 1984). The intensification along this section of the STC is attributed to the southward advection of the warm, saltier water from the juxtaposition of the Agulhas Return Current (Lutjeharms and Ansorge, 2001). Preliminary

results from a recent study (Alcock, 2006) indicated that the geographic position of the STC demonstrated a seasonal pattern. A southward migration of the front was observed in the austral summer and spring months and this was followed by a northward position during the austral autumn and winter months (Alcock, 2006).

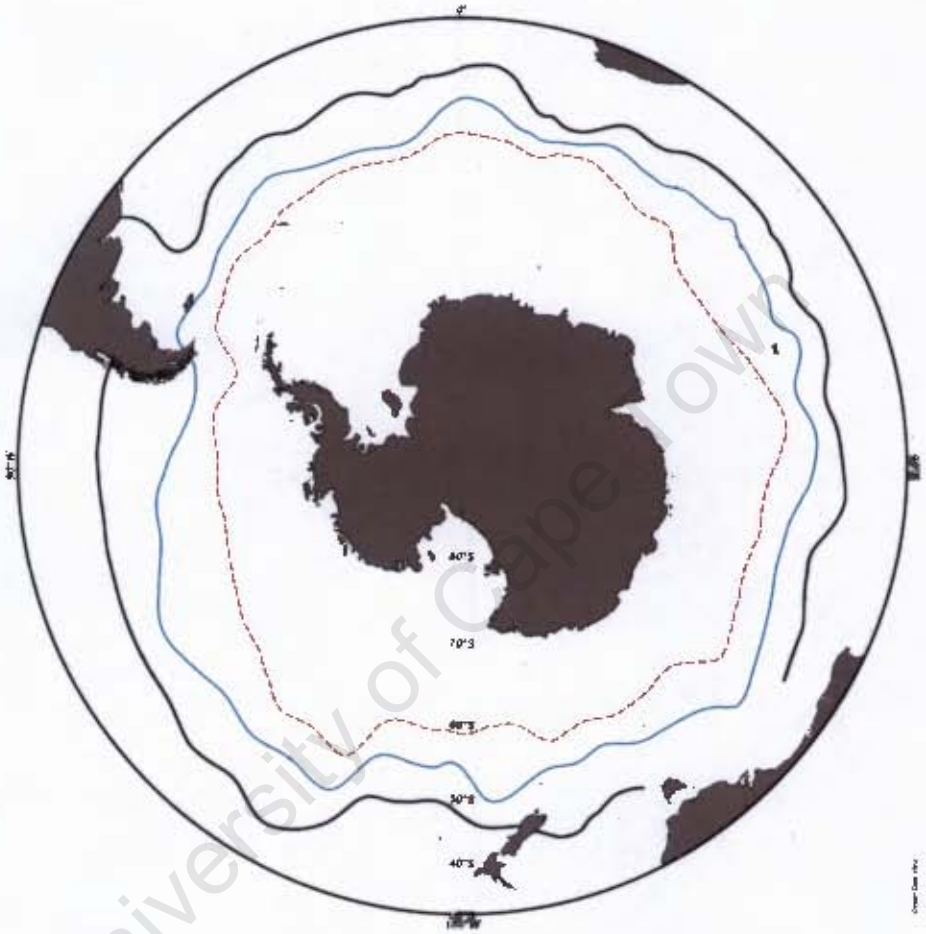

Figure 1. The subsurface (200m) expression of the main frontal bands in the Southern Ocean. Fronts are represented by the following: Black line denotes the 10°C subsurface core of the Subtropical Convergence (STC), blue denotes the 6°C subsurface core of the Subantarctic front (SAF) and the dashed red line denotes the 2°C subsurface core of the Antarctic Polar Front (APF).

Morrow et al. (2004) stated that the STC plays a role in the eddy heat flux/transfer across the oceans through the detachment of meso-scale, cold-core eddies from the Subantarctic zone south of the STC. The cold-core eddies are responsible for moving colder Subantarctic water masses equator-wards and the warm-core eddies advect

warm Subtropical waters polewards. A secondary role of these eddies is apparent in the transfer of salt between water masses. The salt transfer associated with these eddies plays an active role in influencing the physical, chemical and biological structure of the water column across the STC zone (Morrow et al., 2004).

The influence of the STC on biology and climate

The Southern Ocean plays a vital role in influencing climate conditions due to its large extent and the associated influence on the CO_2 levels through the solubility and biological pumps. There are two ways that carbon is taken up by the oceans from the atmosphere;

(i) through the solubility pump where CO_2 in the atmosphere dissolves into the surface water;

(ii) through the biological pump, where CO_2 is taken up during the growth of phytoplankton and converted into biological matter where it either settles and sinks or gets taken up by other organisms (Longhurst, 1991).

The Southern Ocean is considered to be the largest region in the world (Blain et al., 2008) and is said to have a large influence on climate dynamics (Dower and Lucas, 1993). The influence of the Southern Ocean would be larger if it was not for the high-nutrient low chlorophyll-a (HNLC) characteristic that is experienced in this region. The HNLC areas in the ocean have high nutrient (in particular nitrate) concentrations all year round which is necessary for phytoplankton production but does not show the expected or associated high level of primary productivity (Bathmann et al., 2000). The Iron hypothesis suggests that the reason for the lower than expected primary productivity in this region is due to the limited iron supply in these areas (Boyd et al., 2000). A large research drive has focused on this hypothesis and the possibilities of iron fertilization in these HNLC areas to mitigate the increased anthropogenic CO_2 production (Boyd et al., 2007). Recent studies have used radium isotopes to track the iron fertilization and confirmed that iron input stimulates increased primary production (Charrette et al., 2007).

However in 2009, Pollard et al. (2009) showed that the actual amount of carbon sequestered through artificial iron fertilization was considerably less efficient than that of a naturally fertilized region, as previously estimated by Buesseler and Boyd (2003).

Due to the increased mixing and thus increased biological activity recorded in the region of the front, the STC is recognized as an area of increased carbon drawdown from the atmosphere (Metzl et al., 1999) and possibly one of the major carbon sink areas in the world ocean (Dower and Lucas, 1993). Debaar et al. (2005) completed a comparison of eight iron experiments where it was suggested that the carbon drawdown is inversely related to the depth of the mixed layer which defines the light environment. The deeper wind generated mixed layer was especially influential on the biological productivity in the Southern Ocean. It was suggested that the sea surface irradiance, temperature, grazing and lateral patch dilution all play a role in biological productivity and hence carbon drawdown (Debaar et al., 2005). Boyd et al. (1999) suggested that the two main factors controlling diatom growth in the springtime are irradiance and iron. Furthermore, during summer, the irradiance increases and iron, iron-silicate co-limitation or silicate limitation is said to determine the diatom growth (Boyd et al., 1999).

The STC is generally considered as a region of increased biological activity, as can be seen from increased phytoplankton, zooplankton and nekton numbers (Weeks and Shillington, 1996; Froneman et al., 1999). More recently, Llido et al. (2005) have shown, using both satellite observations and a N-P-Z-D (dissolved inorganic nutrient, phytoplankton, zooplankton, detritus), nitrogen based, biological model (Oschlies and Garcon, 1998) coupled with a three dimensional physical model output (Biastoch and Krauss, 1999), that primary production in the vicinity of the STC takes place episodically. The development of the algal blooms appears to be mediated by increased water column stratification (Llido et al., 2005). Additionally, the horizontal advection of phytoplankton, both meridionally and zonally, is likely to sustain the phytoplankton bloom intensity, but

on occasion can cause self-shading and thereby restrain additional growth (Llido et al., 2005).

The STC zone is the region where a unique biological habitat exists as a result of the close proximity of both Sub-Tropic and Subantarctic water masses (Longhurst, 1998). Past investigations (Frontier, 1977; Zubova and Timofeev, 1991) have studied the influence of the convergence of Subantarctic and Subtropical water masses on the development of the local pelagic fauna (Bartle, 1976). An enhanced pelagic community is also evident in the STC region south of Africa (Barange et al., 1998). The diversity and distribution of the phytoplankton, zooplankton (Froneman et al., 1995), fishes (Roberts, 1980) and birds (Pakomov and McQuaid, 1996) across the frontal zone results from the STC acting as a biogeographic barrier (Fiala et al., 2003). The sharp gradients in temperature and salinity and thus density, which are typically associated with the STC, prevent the latitudinal migrations of both warm and cold species across the STC, thus acting as a biogeographic barrier to the distribution and cross-frontal advection of plankton (Froneman et al., 1997).

The need to undertake "ground-truthing" measurements

The STC is a dynamic and complex region and one of global importance in regulating climate due to the increase in biological activity in this region (Dower and Lucas, 1993; Gille, 2002). It is not fully understood how the physical-chemical dynamics and biological enhancements interact with each other and how the mechanics of these processes occur at the STC. Recent studies using remote sensing and physical-biological coupled models, e.g. Llido et al. (2005) and Alcock (2006), have been fruitful but direct observational evidence and our understanding to date still remain rudimentary. Thus it is important to conduct *in situ* hydrographic observations in this region in order to understand the relationship between physical and biological processes. A specific benefit of observational data over remotely sensed data is the ability to accurately measure the

physical and chemical structure throughout the water column. This capability is essential in order to further corroborate remote sensing and model outputs in order to improve our confidence in their findings.

A research survey was conducted north of the Prince Edward Islands in the South-west Indian sector of the Southern Ocean during the austral autumn of 2007. The aim of this survey was to investigate the physical, chemical and biological dynamics of the STC, in the region south-west of Africa.

The aim of this study is to present the data collected during the survey and compare the physical, chemical and biological data with satellite data. In addition, the physical and chemical setting at the time of the survey will be studied to better understand the role the STC has on the biological setting of this region. The objective of the research survey was to study an enhanced primary production event, specifically trying to understand the dynamics, despite the lack of historical observations, and the mechanics controlling the genesis and gradual deterioration. In an area where joint physical and biological data are sparse, any in-situ observations will contribute to the greater understanding of the enhanced primary productivity dynamics occurring at the STC. This study aims to address these uncertainties in the following key objectives.

Key Objectives

(a) An examination of the events preceding and following the survey – to determine whether the region has experienced an enhanced primary production event and whether or not there are any significant meso-scale physical phenomena like eddies in the region.
(b) A description of the physical environment at the time of the survey – to locate the STC, the intensity of the STC and the nature of the geostrophic flow during austral autumn.

(c) Determining how the STC acts as a transitional zone to nutrient types and concentrations – to determine the influence of the STC on the distribution of nutrients across the region, and thus the availability of essential nutrients for primary production.

(d) A description of the biological environment and an examination of the relationship between the nutrients, phytoplankton and mesozooplankton distributions – to determine whether or not the nutrient concentrations correlate to the phytoplankton and mesozooplankton abundance or if there are other factors that are influencing the phytoplankton and mesozooplankton distribution.

Chapter Two - Materials and Methods

In order to address the key aims outlined in the previous chapter, physical, chemical and biological data were collected across the STC. The aim of this study was to compare physical-chemical-biological data collected during the survey, with the aid of satellite data, to aid in the understanding of the role that the STC had on the biological setting of this region.

Data

Data were collected onboard the research and supply vessel the *S.A.Agulhas* during early austral autumn (17 April to 28 April) in 2007. The region surveyed consisted of six transects between 38°- 46°S and 38 – 41°45'E with alternate CTD (Conductivity-Temperature-Depth) and XBT (Expendable Bathythermograph) stations occupied at 15-nautical-mile intervals (Figure 2); Transect line 1 at 38°E, Transect 2 at 38.75°E, Transect 3 at 39.5°E, Transect 4 at 40.25°E, Transect 5 at 41°E and Transect 6 at 41.75°E.

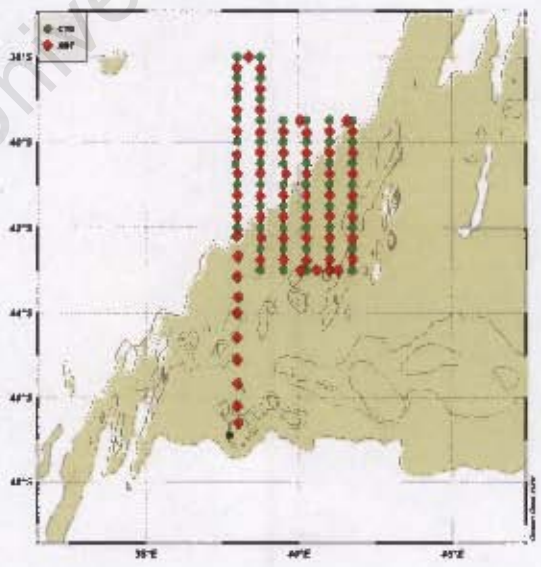

Figure 2: Map showing the location of stations (CTD - green dots) and XBT (red triangles) occupied during the April 2007 survey of the STC region. Bathymetry shallower than 3000 m has been shaded.

Physical and chemical *in situ* data

A total of 54 CTD stations were occupied across the region of interest. Vertical profiles of salinity, temperature and density measurements were obtained with a Seabird SBE 9/11 underwater unit at each station. The descent speed was at a maximum of 1.2m/s and the CTD was deployed to a maximum depth of 1500m. The SeaSave data acquisition and display system was used to collect the CTD data. The CTD was calibrated before and after the survey. The CTD rosette consisted of 10 8-litre Niskin bottles. At each station, water samples were taken on the up-cast, by closing the Niskin bottles, on average, at depths of 1500, 1250, 1000, 750, 500, 150, 100, 75, 50 and 25m. When the CTD rosette was brought on board, the water samples were immediately extracted from the Niskin bottles for oxygen concentration measurement. The volume calibrated iodine flasks were rinsed twice using the drawing tube and then filled to overflow. These samples were analyzed onboard for dissolved oxygen content using the Winkler method. The samples were spiked with 1ml $MnCl_2$ and 1ml NaI and left to stand for approximately 30 minutes. The samples were then spiked with 1ml sulphuric acid and titrated with thiosulphate to determine the oxygen content of the sample. The thiosulphate solution was standardized during the survey. The dissolved oxygen concentration was measured using the Metrohom Dosimate 650 coupled to a 2-beam photometer and operated through a Sensoren Instrumente Systeme GmbH (SIS) software package. Further water samples were collected from the Niskin bottles at each depth to measure the nitrate (corrected for nitrite), silicate and phosphate concentrations. These water samples were taken from the Niskin bottles and were frozen on board. The water samples were later analyzed in the laboratory according to the method described in Grasshof (1983). A few bottles failed to trigger at some stations and some were lost due to entanglement in lanyards. A number of electronic faults with the seabird CTD resulted in transect 2 being sampled with an RBR handheld CTD, to a maximum depth of 750m while these problems were overcome.

In between CTD stations, a total of 66 XBTs were deployed to a maximum depth of 900m within the survey area (Figure 2). The Sippican hand launcher was used to deploy Sippican T7 XBTs. These XBTs were acclimatized beforehand by storing them on the outer deck. The acclimatization of the XBTs was carried out to minimize the possibility of spiking in the surface layers. The XBTs measured the temperature of the water with depth. The data were obtained using the Sippican Mk12 data acquisition system using the NOAA AmverSeas 2000 software interface.

Biological data

Water samples were collected at the surface of the ocean with a Crawford bucket at each station. The chlorophyll-a (Chl-a) concentrations were fractioned by passing 250ml water samples through serial filtration and divided into micro-(>20µm), nano-(2-20µm) and picophytoplankton(<2µm). Chl-a was determined fluorometrically after extraction in 90% acetone for 12 hours (Holm-Hansen and Riemann, 1978). The total Chl-a concentration at 25, 50, 75, 100 and 150m were measured using water samples collected by the CTD. The Chl-a concentrations were then integrated to approximate the amount of areal Chl-a in the region.

The mesozooplankton abundance was determined from samples collected using a Bongo net which was fitted with 200µm mesh size. The net was attached to a Universal Underwater Unit to monitor depth and a mechanical flow meter to determine the volume filtered during each sampling tow. The tows were performed to depths of 200m at night and 300m during the day, to account for the diel vertical migrations of the zooplankton. The zooplankton samples were bottled and preserved in 6% buffered formalin (Froneman et al., 2007).

Satellite data

Sea surface temperature (SST) data and surface chlorophyll-a data were collected from the MODIS AQUA passive satellite instrument via ftp://oceancolor.gsfc.nasa.gov (Feldman, 2007). Level 3 daily, 4km resolution data were collected for the period of 3 April to 12 May 2007 and the SEADAS program was used to extract and view the data (Baith, K., 2001). It was decided to use the QF 2 data for the SST images in order to minimize cloud cover. The satellite data were downloaded and the extraction and visualization of the data was completed using SEADAS.

Surface wind data maps were collected from the QuikSCAT website: manati.orbit.nesdis.noaa.gov/quikscat/. The measurements are taken at 10m reference height from satellite passes, using the NASA/JPL's SeaWinds Scatterometer aboard the QuikSCAT and processed by NOAA/NESDIS (manati.orbit.nesdis.noaa.gov/quickscat).

Daily satellite images were visualised and examined in order to determine whether or not the region had experienced an enhanced primary production event at the time of the survey and whether or not there were any significant meso-scale physical phenomena in the region. A number of the images were not as useful as others due to excessive cloud cover and it was decided that five-day composites of the region would be collated in order to minimise cloud interference. In addition, QuickScat wind data from the website http://manati.orbit.nesdis.noaa.gov/quikscat/ was sourced for the period 3 April – 12 May 2007 and examined.

Analysis of physical, chemical and biological data in relation to the STC

In order to establish the location and intensity of the STC, the nature of its geostrophic flow, as well as the STC's influence on the cross-frontal distribution of nutrients and thus the availability of essential nutrients for primary production, the following method was applied. The criterion for determining the location of the STC according to Belkin and Gordon (1996) is where the 10° C isotherm intersects 200m.

CTD, XBT, Chl-a, mesozooplankton and nutrient data were imported into the Ocean Data View (ODV) program. The temperature, salinity and nutrient data were plotted for each transect line and across the region, at the surface and at depth. The location of the STC according to Belkin and Gordon (1996) is where the 10° C isotherm intersects 200m. Geostrophic currents were calculated and plotted in ODV. Temperature/Salinity diagrams were plotted for notable stations. Mixed layer depth (MLD) was identified by a 0.2°C change in temperature from a reference depth of 10m (DeBoyer et al.,2004). DeBoyer et al. (2004) conducted a comprehensive study on the MLD determining specific criteria to describe the MLD. The study concluded that a change in temperature of 0.2°C with depth is a suitable criterion for determining the MLD. A reference depth of 10m from the surface was used. Density, Brunt Vaisala and Potential temperature were calculated using ODV and plotted.

Statistica 8 (Statsoft 2002) was used to investigate relationships between physical, chemical and biological variables, and to determine whether the nutrient concentrations were correlated with phytoplankton and mesozooplankton abundance, or if there was another factor that was influencing the phytoplankton and mesozooplankton distribution. Nutrient. oxygen and Chl-a data were integrated to 150m. Mesozooplankton data were transformed using the root-root method, i.e. sqrt(sqrt(ind/m^2)) (Statsoft, 2002). The data were analysed to check for normality and equal variance using the Kolmogorov-Smirnof

test and the Levene's test, respectively. Pearson's product moment correlations were conducted on the data to assess the relationship between the variables.

Criteria for water mass identification

The data were divided into different water masses identified by their salinity and temperature characteristics. Subtropical Surface Water (STSW) has characteristic salinities between 35.5psu and 34.6psu (Darbyshire, 1966) and lies between 15 and 24°C and Subantarctic water masses display a maximum subsurface salinity of 34.5psu and temperatures below 14°C. Mixed water has salinity between 35.2 and 35.3 with temperatures between 14°C and 17°C. These water masses were then tested for significance of difference using the biological and nutrient data. A One-way Model 1 ANOVA was performed on these data. Further analysis between the variables within these water masses was conducted by using Pearson's product moment correlation.

A post hoc test, Tukey HSD test, was performed for the grouped data and Bonferroni adjustment of significance values was completed for all the statistical analyses.

In accordance with this method, we have confidence in drawing comparisons between the biological, chemical and physical components collected.

Chapter Three - Results

The STC is a dynamic and complex region and one of global importance in regulating climate through the heat and mass exchange across the oceans and associated biologically driven carbon sink (Gille, 2002; Dower and Lucas, 1993). It is not fully understood how the physical-chemical dynamics and biological enhancements occur and interact with each other or what the mechanics of these processes are at the STC. Results presented here address and describe features and interactions of the physical-chemical and biological variables during the austral autumn.

Physical setting of the survey region

Satellite imagery of Sea Surface Temperature (SST) and Chl-a were examined over the survey period (Figure 3). The broader region showed high variability associated with the STC as a result of extensive meandering, pulsing and/or pinching off of a cooler Subantarctic water masses northwards (Figure 4). The area between 36ºS and 46ºS and to the west of the region at 25ºE - 50ºE demonstrated the most variability with an extensive train of meanders and filaments extending eastwards. Satellite data images of SST were examined over the period 3 April - 12 May 2007. Initially, the satellite data showed little evidence of meandering over the survey region. The temperature and Chl-a gradients followed the latitudinal plane. Over the next five days (8 - 12th April), meandering of the STC was evident and Chl-a was almost absent. The following five days (13 - 17th April) showed an increase in Chl-a concentration associated with the generation of a cold filament over the survey region. The increase in Chl-a continued over the following five days(18th – 22nd April) during the survey and was associated with this colder feature that was evident at 38°-39°E, 38° - 40°S. The increase in production associated with this feature gradually dispersed (23 - 27th April 2007) as the cold water became entrained northwards at 37

- 38°S. The following days showed a decrease in Chl-a levels over the region. The problem of cloud cover was very pronounced at this point and continued to be so until the 12th May 2007.

A composite of the SST satellite data showed a colder (<18°C) water filament extending northwards along the 38°E transect, which corresponded to the survey findings. Figure 3 shows the cold water as a filament extending northwards to 37°S for the period 17-21 April 2007. Data from transect 1 (38°E), which extended along the filament, showed temperatures ranging from a maximum of 19.26°C at 40.12°S to a minimum of 6.72°C at 46°S. A region of cooler water was evident where the surface temperature dropped to 16.2°C at 39.24°S and rose to 18°C at 38°S, to the north west of the survey region.

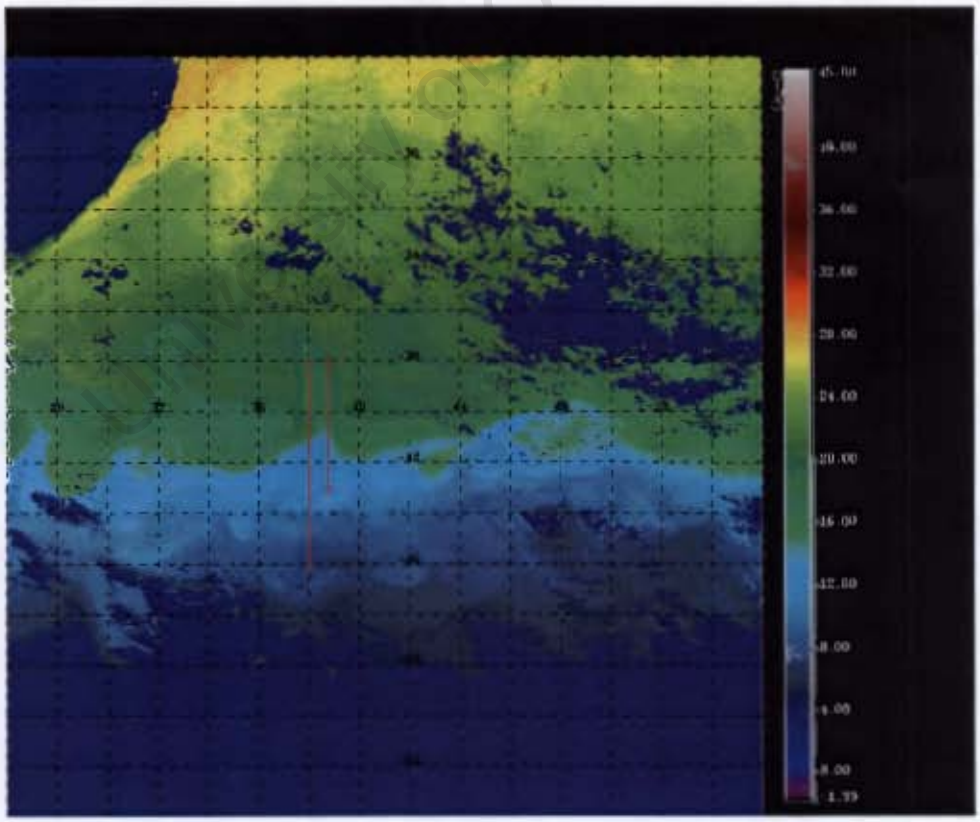

Figure 3: Composite image of mean of SST over the period 17-21 April 2007 showing transect 1(38°E) on the left and transect 2 (38.75°E) on the right

The geostrophic currents (Figure 4) further corroborated the SST findings with a distinct mixture of both anti-cyclonic and cyclonic flow associated with the filament extension. An anti-cyclonic flow was observed associated with the warm feature at approximately 40°S and 38°E.

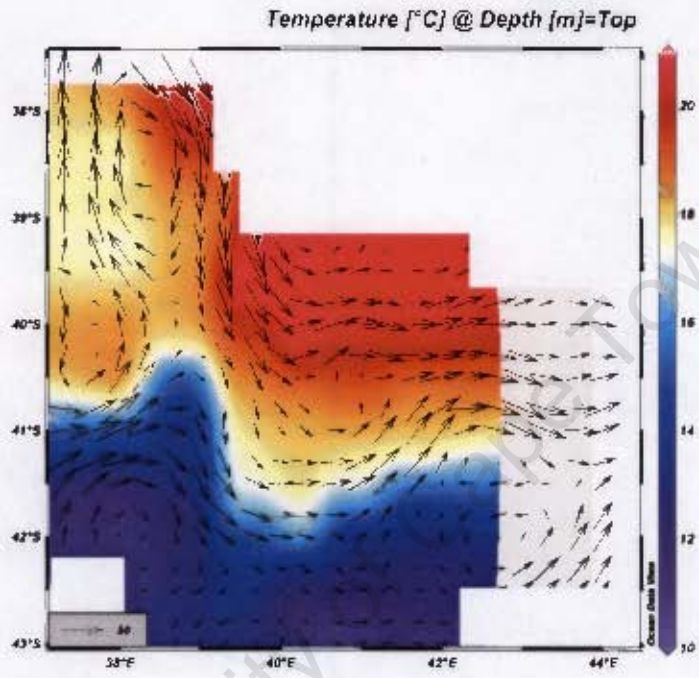

Figure 4: Geostrophic currents (cm/s) overlaid on SST for the survey region

Geostrophic velocities for transect 1 (Figure 5a) and transect 4 (Figure 5b) were examined. These two transects represented the different sections of the region and were referenced to 1500m; Transect 1, the area where the STC was further north and where the colder feature was evident and transect 4, where the STC was further south and no features were evident. Transect 1 showed the STC at 41°S with easterly velocities between 40-50cm/s. In contrast, further north, the velocities were slower, between 0 and 10cm/s, from 40.25°S – 39°S and exhibited a westerly flow. Along transect 4 easterly velocities associated with the STC had a maximum speed of 50cm/s at 40.5°S and slowed to around 10cm/s around 42.5°S. The maximum depth of the fast current was approximately 700m, at 20cm/s, and became shallower

further south. It was evident that there was a large amount of variability in the position, direction and speed of the currents over the survey region.

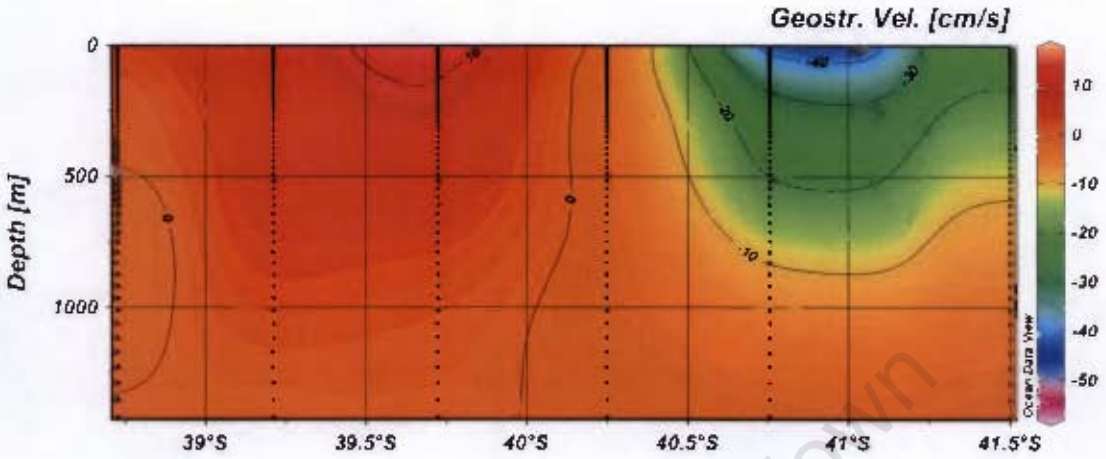

Figure 5 a: Vertical section showing the geostrophic velocities (referenced to 1500m) in cm/s for transect 1 (38°E).

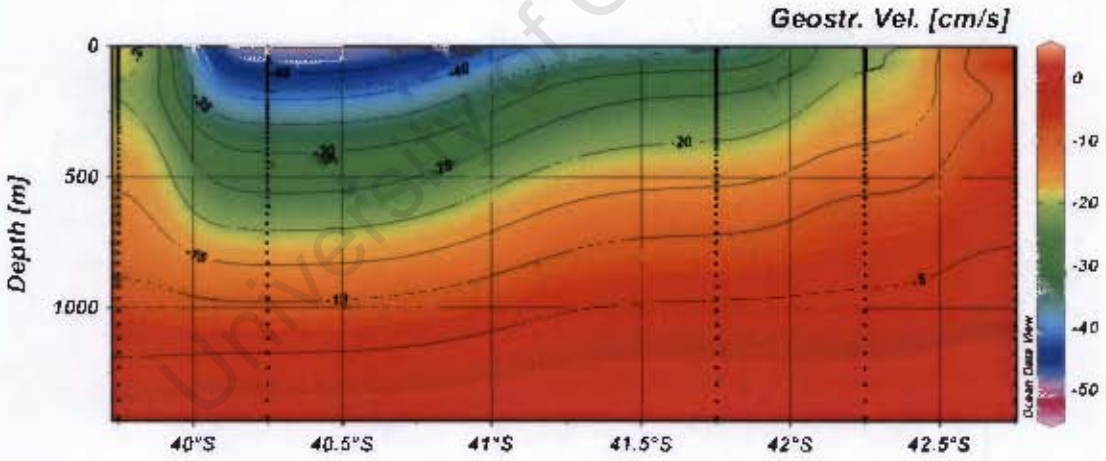

Figure 5 b: Vertical section showing geostrophic velocities (referenced to 1500m) in cm/s for transect 4 (40.25°E)

The STC was positioned at 41°S and 38°E along transect 1, and then appeared to shift southwards to approximately 42.25°S and 39.5°E along transect 3. It meandered considerably throughout the survey as seen by its subsurface expression of 10°C (Figure 6a). The Agulhas Retroflection Current was evident from 39.5°E – 41.75°E and 39.5°S – 40.5°S. The salinity plot (Figure 6b) also highlighted the nature of the

boundary, typical of the STC, between fresher Subantarctic waters and saltier Subtropical water masses to the north. The survey region ranged from Subtropical waters to the north into the Subantarctic region. As a result the following water masses and associated temperature and salinity signatures were encountered.

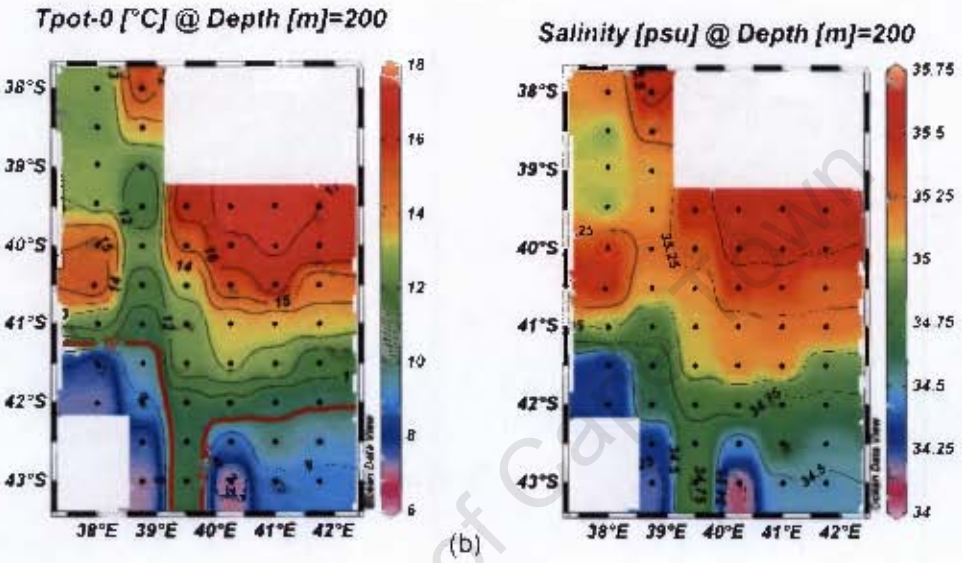

Figure 6: Potential temperature (°C) (a) and salinity (b) measured in practical salinity units (psu) at a depth of 200m within the survey area. The black dots represent the station positions in the survey area.

Brief overview of water masses associated with this region

Subtropical Surface Water (STSW) has a characteristic temperature range of between 15°C and 24°C and salinities between 35.5psu and 34.6psu (Darbyshire, 1966).

Agulhas Water (AW) temperatures range from 14 to 17°C and salinity between 35.2psu – 35.35psu (lower in salinity due to the river run-off from the continent) (Darbyshire, 1966; Holliday and Read, 1998).

Subantarctic Surface Water (SASW) and Antarctic Surface Water (AASW) (Holliday and Read, 1998) vary in characteristics seasonally and zonally – both exhibit lower temperatures in winter and lower salinity further south due to the input of fresher water via precipitation and ice melt water (Deacon, 1937; Read and Pollard, 1993).

Water masses observed during this survey

Subantarctic water masses display a maximum subsurface salinity of 34.5psu while Subtropical water masses have salinity values of a minimum 35.4psu. The STC showed the characteristics of SASW water masses to the south of the survey region at approximately 41°S, STSW to the far north of the survey region and an area of mixed water exhibiting salinity values between the two water mass saline characteristics. These temperature and salinity characteristics of the different water masses mentioned above are used to divide the collected data into the different water masses for analysis.

Figure 7 further corroborated these temperature and salinity characteristics. The T/S diagram (Figure 7) of Station 91 at 39.5°S, Station 99 at 41.5°S and Station 105 at 43°S along 42°E showed the characteristics of the different water masses. Figure 7 further highlights the strong physical signature associated with the STC, which separated the Subtropical zone from the Subantarctic zone.

Station 91 had characteristics typical of Subtropical water, approximately 20°C and 35.4psu. Station 105 is characteristic of Subantarctic waters, approximately 12°C and 34.5psu with a maximum subsurface salinity of 34.65psu. Station 99 showed a mixture of these water mass characteristics between AW, Indian STSW and Atlantic STSW and water from the Subantarctic zone (Read and Pollard, 1993).

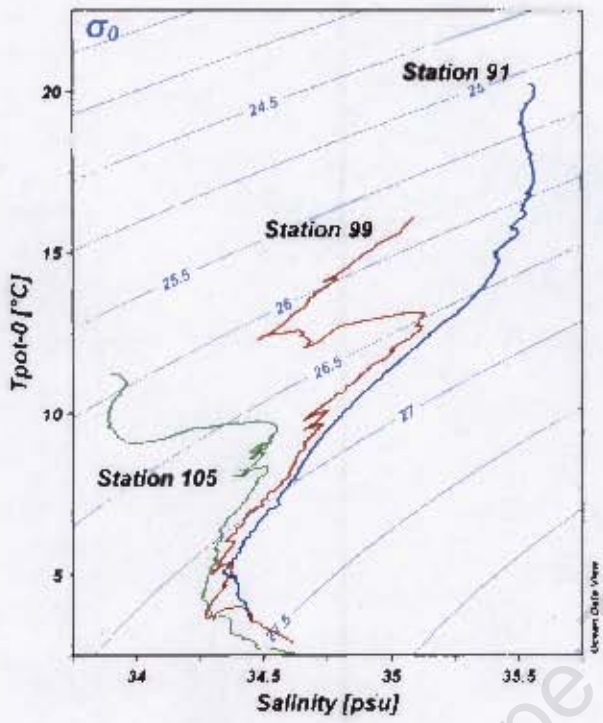

Figure 7: T/S diagram of three stations, 91, 99, 105 along transect 6 (41.75°E) and thus typical of the different frontal zones encountered along this transect

The colder feature was also evident in the temperature section along transect 2 at 38.75°E (Figure 8a). The 12°C isotherm showed that the colder water mass was present at the surface at 40.75°S and extended further south to 43°S. The 16°C isotherm was at the surface at approx 40.25°S. This shows the extent of the northward movement of the colder water along transect 2. Transects 2-6 (not shown here) exhibit 16°C at the surface at much lower latitudes (41.5°S-42°S) than transects 1 and 2 (Figures 8a and b). Transect 1 (Figure 8b) showed the colder feature (<18°C) at 40.75°S and again further north between 39.75°S and 38°S.

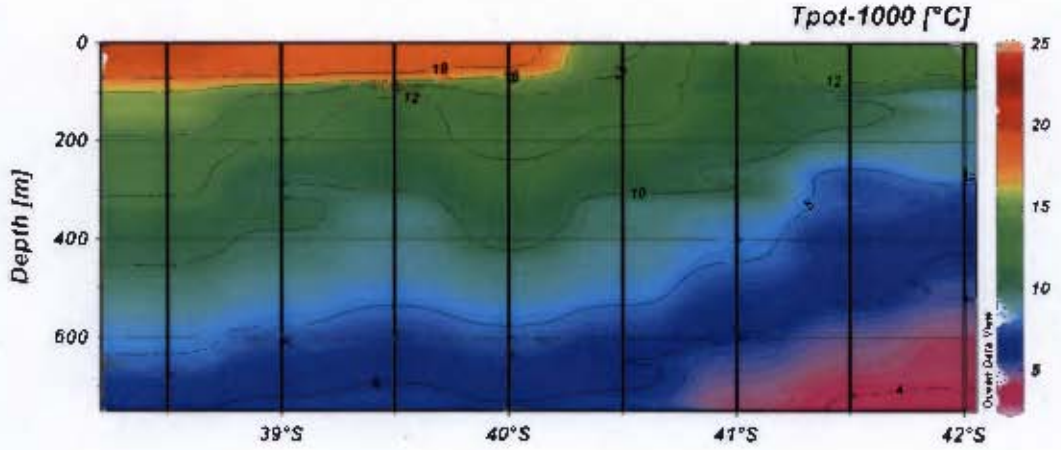

(a)

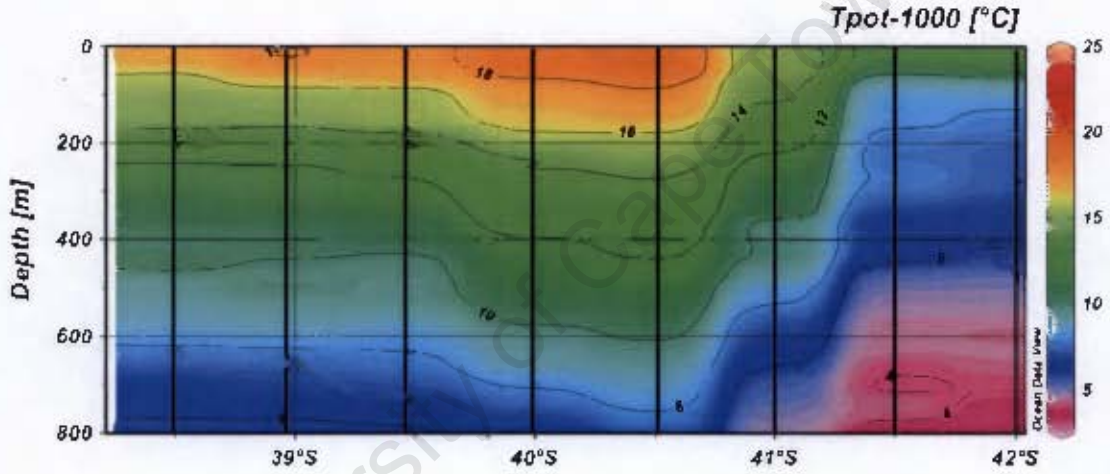

(b)

Figure 8: (a) Potential temperature (°C) is displayed for transect 2 (38.75°E) (b) Potential temperature (°C) is displayed for transect 1 (38°E) with depth (reference pressure of 1000db). The sampling frequency for the stations are displayed with black vertical lines. See figure 2 for transect lines and appendices for other transect line figures.

An area of increased temperature at 38°E between 39.75°S and 40.5°S including an increase in salinity was evident (Figures 6a and b). In addition, a line of decreased temperature (12°C) and salinity (35.25psu) along 39°E along 38.5° - 41°S was observed at the subsurface level.

The density of the water (at 200m) over the survey area is represented in Figure 9b. This region was characterised by water of a lower density (26.4kg/m^3) which lies to the north east of the survey region and at the feature located at 40°S and 38°E. A tongue of dense water, above 26.6 kg/m^3 between 38° and 39°E was evident. The area to the south of the STC was associated with denser water above 26.4 kg/m^3. The Brunt Vaisala frequency, which measures the frequency at which a vertically displaced particle will oscillate within a statically stable environment (i.e. the vertical stratification), for the survey region is represented in Figure 9a. The region to the south of 41°S shows Brunt Vaisala values of less than 1-1.5 cycles/hr across the survey region. To the north of 41°S the Brunt Vaisala frequencies range from 2 – 3cycles/hr, with the exception of the region at 38.5 – 39°E where the values are between 1-1.5cycles/hr (Figure 9a).

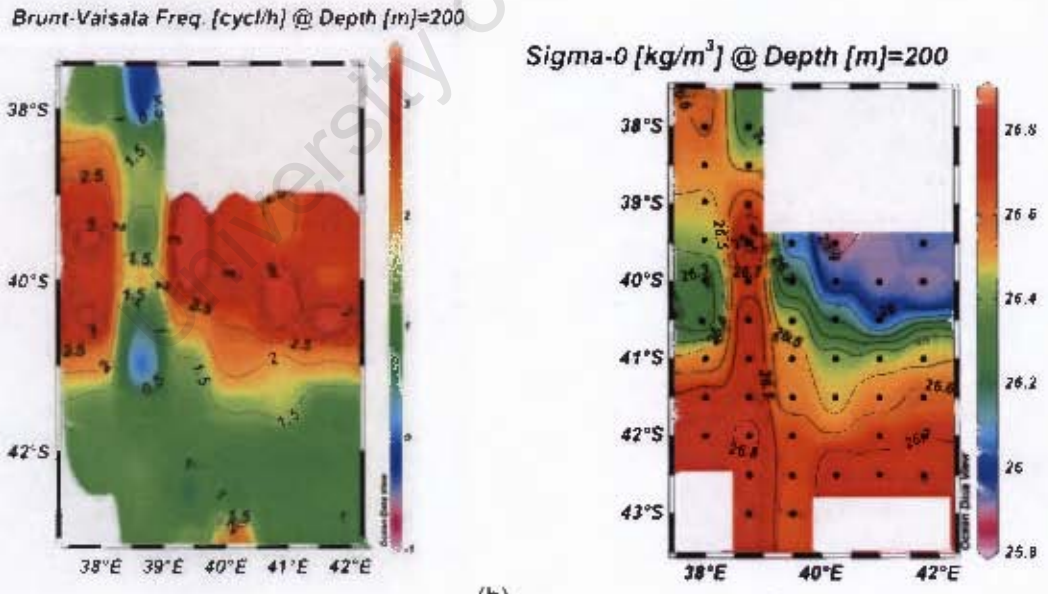

a) (b)

Figure 9: Brunt-Vaisala (a) and Density (b) surface plots at the depth of 200m, black dots represent station positions

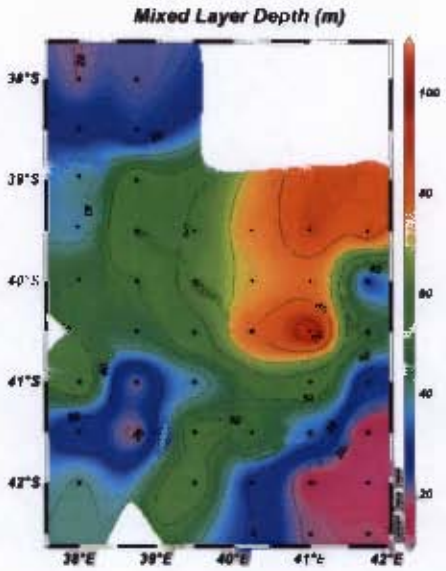

Figure 10: Mixed layer dept (MLD) in metres across the six transect lines of the survey region.

The deepest MLD of 101m was measured at 41.5°S and 41°E and the shallowest MLD, 11m, at 42°S and 41.75°E. Transect 5 (41°E) showed the highest and transect 3 (39.5°E) showed the lowest variability in the MLD (Figure 10). The MLD in Subantarctic water was observed to be significantly shallower than in the Subtropical and Mixed water ($F=9.213$; $p<0.001$).

Quikscat wind data were sourced for the survey region and showed high wind speeds, between 25 and 40 knots two days before the survey (15th April 2007). The wind speeds over the survey period reduced to between 5 to 15 knots. The wind speed increased again from the 28th of April to 30th April to between 25 and 45 knots.

Chemical setting of the survey

The concentrations of the nutrients, silicate, nitrate, phosphate and oxygen were measured through the water column. The integrated nitrate, phosphate, silicate and oxygen concentrations (Figure 11) over the survey region are shown in Figure 11 (a-d). Nitrate concentrations ranged from 0.6 µM to 16.1µM. The silicate concentrations ranged between 2.5µM and 10.6µM. The phosphate concentrations ranged between

0.25 µM and 1.54 µM. Oxygen concentrations ranged from 2.8ml/l and 7.4ml/l. Oxygen, nitrate and phosphate concentrations were higher to the south of the survey region and south of the STC. The STC seemed to act as a barrier to nutrient transfer. Silicate concentration, however, did not show the same distribution patterns as the other nutrient concentrations. Silicate concentration did not show any link to the position of the STC as the silicate concentration was varied across the entire region. The lowest silicate concentration was to the south of the STC. Higher levels of phosphate, silicate and nitrate concentrations were also evident at 38°S and 38°E.

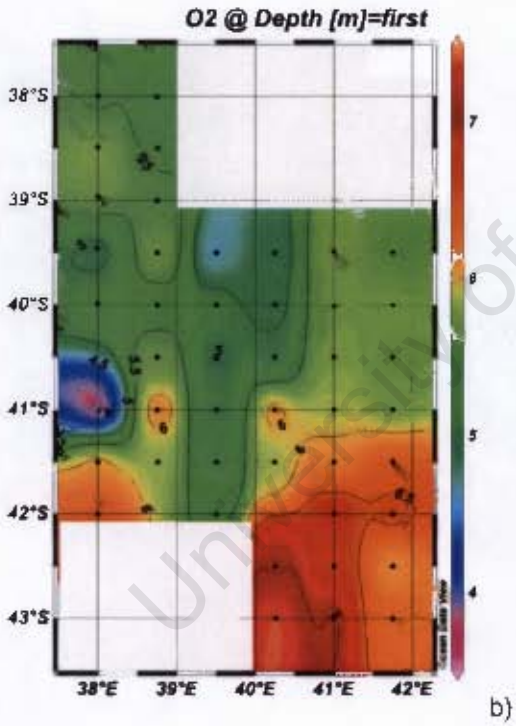

a)

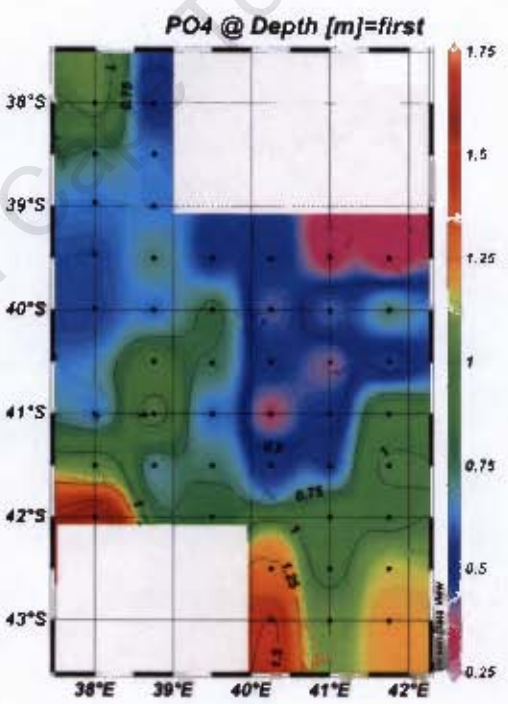

b)

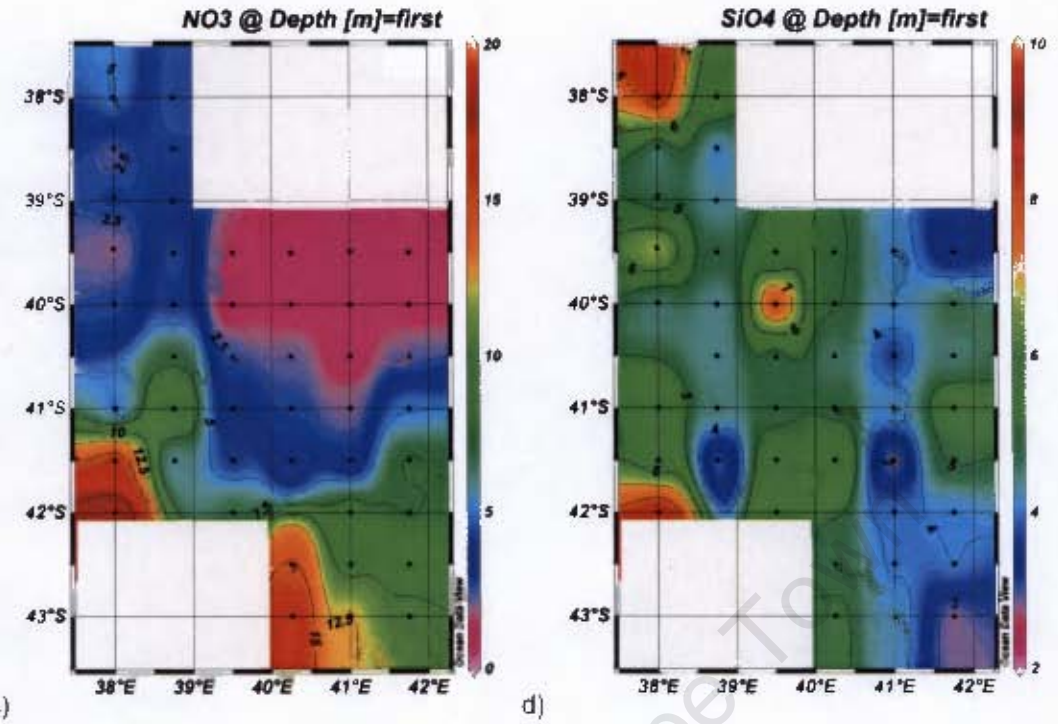

Figure 11 Integrated Oxygen (a), measured in ml/L, phosphate (b), nitrate (c) and silicate (d) measured in µM, concentrations across the entire survey region.

Vertical sections of the nutrients and oxygen were plotted in ODV (Appendix 6). The nutrient concentrations displayed the following characteristics; nitrates, silicates and phosphates increased in concentration with depth while oxygen concentration decreased with depth. Nitrates and phosphate concentration appeared to follow the isotherms in most transects.

Biological Setting of the survey

The surface Chl-a concentration ranged from 0.03 to 0.42µgChl-a/l while that of the integrated Chl-a ranged from 12.83 to 40.07mgChl-a/m^2. Spatially, there appeared to be a higher integrated Chl-a concentration to the north-west, 39°S and 38°E, and to the south east, south of 42°S and 40-42°E, of the survey region (Figure 12a).

The integrated mesozooplankton abundance ranged from 3935 ind/m^2 to 308521ind/m^2 at 39°S and 38°E (Figure 12b). There appeared to be a region of higher abundance to the north west of the survey region around 38 – 40°S and 38 – 39°E.

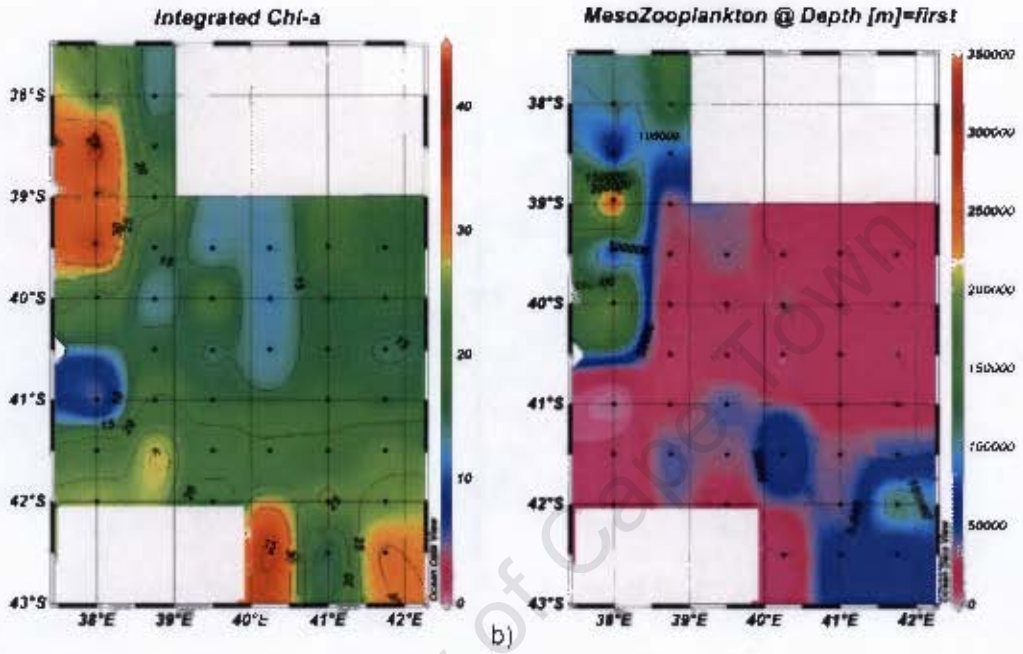

a) b)

Figure 12. Integrated Chl-a concentration (a) (mg/m^2) and mesozooplankton abundance (b) (ind/m^2) over the survey region.

The satellite image showing the Chl-a concentration (Figure 13) also showed a plume of comparatively higher Chl-a concentration over this period at 38° - 40°S, 38°- 39°E. The maximum value of Chl-a measured was 0.46mg/m^2 at 45.12°S and the minimum was 0.18mg/m^2 around 41.25°S. Chl-a value rose up to 0.42mg/m^2 at 38.3°S (Figure14).

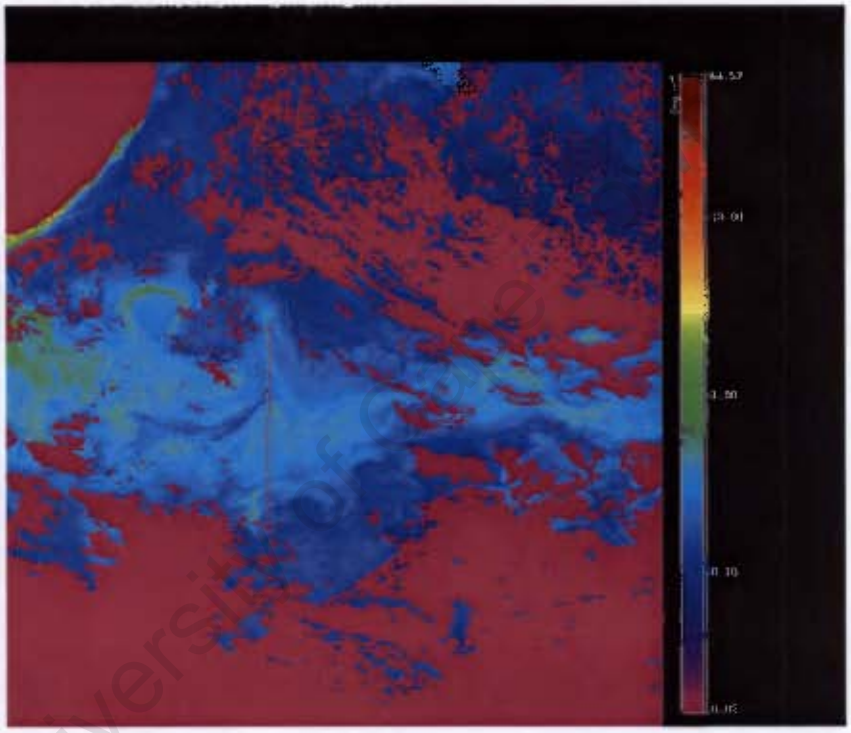

Figure 13: Satellite image showing Chl-a mean values for 17 – 20 April 2007 and red line represents the transect line 1.

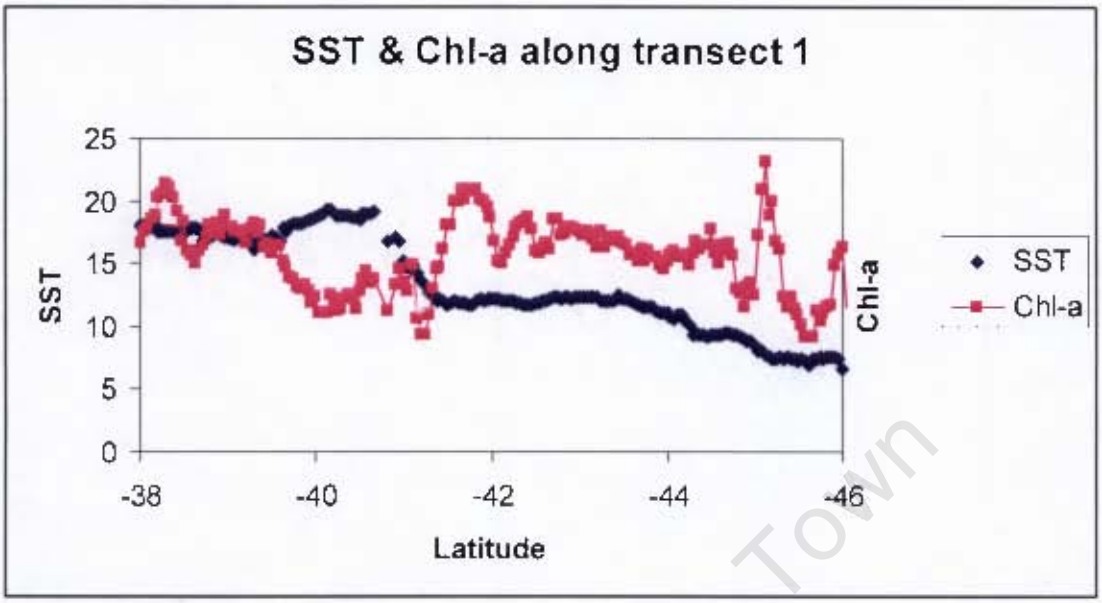

Figure 14: SST and Chl-a mean values measured by satellite remote sensing for the period 17-21 April 2007.

Relationships between the physical, chemical and biological variables

The relationships between the physical, chemical and biological variables measured over the survey showed varied correlations (Appendix 1). The Bonferroni correction was applied to the statistical results (Table 2). The Bonferonni correction for the significance values of the correlations were calculated as follows. Seven correlation tests were performed for each water mass. The accepted significance level is 5%. In order for a result to be classified as significant, the probability of getting the result the chance for the significant result should be 0.05/7 = 0.007. The Bonferronni correction therefore states that the highest significant value (first rank) seen in the statistics table is only significant if $p<0.007$. For the second most significant result, seen in the statistics table, is only significant if $p<0.05/6 = 0.008$. The third most significant result is only significant if $p<0.05/5 = 0.01$. Table 2 shows these corrected p values.

Table 2: Bonferroni correction for each significance value (p value)

Significance rank (First is the smallest p value)	**Corrected p values for α =0.05**
First	0.05/7 = 0.007
Second	0.05/6 = 0.008
Third	0.05/5 = 0.01
Fourth	0.05/4 = 0.0125
Fifth	0.05/3 = 0.0167
Sixth	0.03/2 = 0.025
Seventh	0.05/1 = 0.05

Entire survey region

There was a significant negative correlation between integrated Chl-a concentration and MLD (r=-0.3605, p=0.011) (Figure 15) over the entire survey region. The correlation between integrated Chl-a concentration and phosphate concentration was significant (r=0.512, p=0.011). Integrated Chl-a concentration and temperature at 10m (r = -0.586, p<0.001) was also significant. Integrated mesozooplankton abundance was correlated with MLD (r=-0.293, p=0.049) but after the Bonferronni correction, this result was not significant. Oxygen concentration correlated significantly with temperature at 10m (r=-0.32, p=0.028), with phosphate concentration (r=0.559, p<0.0001) and with nitrate concentration (r=0.656. p<0.0001). The correlation between phosphate concentration and nitrate concentration was highly significant (r=0.8779, p<0.0001). Nitrate concentration and temperature at 10m correlated significantly (r=-0.882, p<0.0001). Phosphate concentration and silicate concentration correlated significantly (r=0.346, p=0.02).

Phosphate concentration and MLD correlated significantly (r=-0.589, p<0.0001). Phosphate concentration and temperature at 10m correlated significantly (r=-0.764, p<0.0001). MLD and temperature at 10m (r=0.532, p<0.001) also showed significant correlation.

Figure 15: Scatter plot showing the MLD versus Integrated Chl-a concentration over the survey area

Using the temperature and salinity characteristics of the different water masses stated earlier, the survey region was divided into the three different water masses. Statistical analyses were performed to determine if there were any significant relationships between the variables within and between the water masses.

Between Water Masses

In order to complete a one-way ANOVA test for differences between water mass groups' means, the assumption of equal variances had to be tested. A Levene's test

for homogeneity of variance was completed (Appendix 2). Levene's test showed that the nitrate concentration had to be rejected for the ANOVA as the variances were significantly different ($F=17.661$, $p<0.0001$). The rest of the variables had similar variances and thus were included in the ANOVA. The ANOVA table for univariate results is located in the appendices (Appendix 3a and b). The multi-variate results showed significant differences between the water mass groups ($F\ (14,72)=7.365$, $p<0.0001$).

The Tukey HSD test was performed on the selected variables in order to assess which groups showed significant differences between the water mass group means (Appendix 4). Mean phosphate concentration for Subantarctic water mass was significantly higher than Mixed water masses ($p=0.0001$) and Subantarctic water mass was significantly higher than the Subtropical ($p=0.0001$) water masses. Oxygen (mean) concentration in Subantarctic water mass was significantly higher than the Mixed water mass ($p=0.0002$) and also significantly higher than the Subtropical water mass ($p=0.0001$). Integrated Chl-a (mean) biomass in Subantarctic water mass was significantly higher than the Subtropical water mass ($p<0.0001$); Mixed water mass integrated Chl-a (mean) biomass was significantly higher than the Subtropical water mass ($p=0.02$). MLD (mean) was significantly shallower in the Subantarctic water mass compared to the Mixed water mass ($p=0.02$) and Subantarctic water mass MLD (mean) was also significantly shallower in comparison to Subtropical water mass ($p<0.001$) MLD (mean).

Within water masses

Within the Mixed water, the following significant correlations were detected; Phosphate concentration and silicate concentration ($r=0.59$, $p=0.01$); phosphate concentration and nitrate concentration ($r=0.764$, $p<0.0001$); phosphate concentration and MLD ($r=-0.685$, $p=0.002$). The Subtropical water displayed the

following significant correlations; phosphate concentration significantly correlated to MLD ($r=-0.063$, $p=0.018$) and oxygen significantly correlated to integrated Chl-a ($r=0.068$, $p=0.018$). The Subantarctic water showed a significant correlation between phosphate concentration and nitrate concentration ($r=0.843$, $p<0.0001$).

See appendix 5 (a-g) for tables containing relevant statistical values.

Chapter Four - Discussion and Conclusion

Using the physical-chemical-biological data collected during the survey with the help of satellite data we are able to better understand the role that the STC has on the biological setting of this region. The results from the data analysis are discussed here.

A. Variability and position of STC shown by satellite imagery and in-situ data

The variability of the STC (Joyce and Patterson, 1977; Lutjeharms, 1985; Belkin and Gordon, 1996) in the south Indian Ocean sector of the Southern Ocean was confirmed during this study. The broader region (26 – 56°S, 26 – 56°E) showed high variability associated with the STC as a result of extensive meandering, pulsing and/or pinching off of cooler Subantarctic water masses northwards (Figure 3). The area between 36ºS and 46ºS and to the west of the region at 25ºE - 50ºE showed the most variability with an extensive train of meanders and filaments extending eastwards. The satellite data showed a decrease in SST in the survey region specifically to the north west of the survey region. A distinct plume or filament of cooler water was seen between 38-39°E. The feature developed from the 8th April and became very pronounced by the 17th April and dissipated by the 24th April. The quick evolution and dissipation of this feature demonstrates the temporal intensity of the dynamics in the region.

The *in situ* data confirmed that the STC position meandered considerably during the survey period. The STC is usually situated further north but during the survey the STC meandered south for the majority of the time. The STC was positioned further south than usual for this region as it is usually situated at approximately 41°S (Belkin and Gordon, 1996). The position of the STC in the Atlantic and Indian Oceans is said

to correspond to the maximum wind stress curl in the Southern Ocean (Peterson and Stramma, 1991). A possible explanation for this southward movement may be due to the influence of other fronts or currents in the region.

The Agulhas Retroflection Current (ARC) was present in the survey region, located to the north of the survey region, at 40°S and between 40 - 42°E. Belkin and Gordon (1996) found that the ARC and associated Agulhas Front (AF) forced the STC southwards to 42° - 43°S in this region. The SST gradient for the mean SST over 17th - 21st April across the STC was 0.04°C/km at approximately 41°S and 38°E. The intensification along this section of the STC is attributed to the southward advection of the warm, saltier water from the juxtaposition of the ARC (Lutjeharms and Ansorge, 2001). The evidence found in this survey corroborates the theory that the position of the ARC influences the position and intensity of the STC.

Another possible reason for the southward meander of the front may be due to the topography associated with the region. The South West Indian Ridge bisect the survey region diagonally (Figure 2). The interaction between the bottom topography and the geostrophic currents creates increased levels of meso-scale variability (Lutjeharms et al., 2002)

B. Anomaly events observed in the STC region

There were two features evident along the 38 – 39° E transects – one being the warm core eddy-like feature and the other being the cold filament that was identified in the satellite data. The colder feature was observed at 38.75°E and was also seen in the satellite imagery (Figure 3). This feature was expressed in the density and Brunt Vaisala figures (Figures 9a and b). The colder region was associated with denser water than its surrounds and a lower Brunt Vaisala frequency. This water

presented a more stable region, where the MLD remained between 20 and 60m. The geostrophic surface currents were weaker in this region. The temperature section along this transect showed that the cool 12°C water remained above 250m and the surface temperatures remained under 18°C at 40.75°S and again further north between 39.75°S and 38°S. The wind direction corresponded to the direction in which this cold feature propagated. The wind strength weakened during the survey and the wind direction was very changeable. The feature did not last for the length of the survey, hence it is inferred that the wind influenced or aided in the formation and maintenance of the filament/plume. Thus this colder water could have propagated northward by the intense wind event, prior to the survey.

An area of warmer (14°C) and more saline (35.3psu) sub-surface water along 38°E between 39.5°S and 40.5°S was evident (Figures 6a and b). The satellite data showed an area of increased temperature to the west of the survey region, an eddy like feature. This warm feature was the eastern most part of an anti-cyclonic warm feature.

The geostrophic currents further corroborate the SST findings with a distinct mixture of both anti-cyclonic and cyclonic flow associated with the filament extension. An anti-cyclonic flow was observed at the warm feature at approximately 40°S and 38°E and cyclonic circulation was associated with the cold feature.

Morrow et al. (2004) stated that the STC plays a role in the eddy heat flux/transfer across the oceans through the detachment of meso-scale, cold-core eddies from the Subantarctic zone south of the STC. These eddies are responsible for moving colder Subantarctic water masses equator-wards or the detachment of meso-scale, warm-core eddies advecting warm Subtropical waters polewards. A secondary role of these eddies is apparent in the transfer of salt between water masses and the influence this

activity plays not only on the physics but also on the nature of the biological and physical-chemical structure (i.e. nutrients) in this area (Morrow et al., 2004).

The different water masses with the associated unique temperature, salinity and nutrient characteristics including Subantarctic water, Subtropical water and Agulhas water/Mixed water were evident in the survey region. The differences between these water masses are explored here.

C. Biology and nutrient distribution and their association with water masses

Spatially, a higher integrated Chlorophyll-a (Chl-a) concentration to the north-west, 39°S and 38°E, and to the south east, below 42°S and 40-42°E, of the survey region was observed (Figure 11a). A region of higher integrated mesozooplantkon abundance in the north-west of the survey region, 38 – 40°S and 38 – 39°E, was also observed (Figure 11b).

Integrated Chl-a concentration in Subantarctic water was significantly higher than in Subtropical waters. Integrated Chl-a concentration in Mixed water was significantly higher than in Subtropical water. Where the integrated Chl-a levels were higher, we might expect higher phytoplankton biomass. Integrated mesozooplankton abundance showed no significant difference between the water masses. An investigation into why the Subantarctic water mass exhibited a significantly higher phytoplankton biomass could be as a result of a number of reasons. Some of the more plausible reasons will be explored in this discussion.

Subantarctic water had significantly higher oxygen and phosphate concentrations than Mixed ($p<0.0001$) and Subtropical ($p<0.0001$) water masses. The integrated Chl-a concentration over the entire region correlated to phosphate ($r=0.5$, $p=0.001$).

We are therefore able to infer that the increased phytoplankton biomass could be influenced by the increased phosphate concentration occurring south of the STC. The associated oxygen concentration occurring south of the STC is likely to be as a result of the oxygen that is given off by the phytoplankton. The HNLC theory explained in the introduction states that the Subantarctic waters should have increased nutrients, observed here, but should have lower Chl-a concentration than that of the Subtropical water (Bathmann et al., 2000). The results of this study for integrated Chl-a biomass are thus in conflict with the HNLC theory and hence we investigate the physical dynamics in search of clarification.

D. Physical dynamic influence on nutrients and biology

The availability of nutrients for phytoplankton production plays a role in determining the extent of the phytoplankton production (Read et al., 2000). Read et al. (2000) stated that diatoms prefer high silicate to nitrate ratios. Blue-green algae are associated with low nitrate to phosphate ratios (Howarth, 1988) and dinoflagellates are associated with low nitrate to phosphate ratios (Margalef, 1978). Read et al. (2000) suggested that the nutrient ratio values in the surface waters are for the most part due to the uptake by phytoplankton whereas in deeper water due to re-mineralisation processes. A study on phytoplankton assemblages carried out during the survey (conducted by Froneman et al. (2007)) showed that the surface Chl-a concentration was dominated by the pico and nano-size phytoplankton classes (between 81% and 93% in total) and microphytoplankton contributed less than 10% of the total pigment. These smaller phytoplankton are usually more evident in regions where there are limited nutrients and stratification, where there are few silicates and other important nutrients such as iron for diatom growth. These smaller classes are able to use the recycled nitrogen and phosphorous from ammonia and urea for production. The study indicated that the majority of the survey region was not in a

bloom state and that it was most likely in a state of mixing out and post bloom (Froneman et al., 2007). Evidence of increased chl-a in the north-west of the survey region, associated with the cold filament, appeared to be part of a short-lived algal bloom.

A major contributing factor to increased biological activity, particularly increases in phytoplankton biomass, is that of mixing across the frontal zone, where the warm, oligotrophic, nutrient poor and well stratified waters to the north of the STC interact with the cold, nutrient rich (except silicates), well-mixed water to the south (Weeks and Shillington, 1996). The influence of eddies play an important role in the transportation of heat, salinity, nutrients and influences the biological activity across the frontal zone (Froneman, 1999). The significantly higher integrated Chl-a concentration observed in the Mixed water (than Subtropical water) occurring in our survey region illustrates the importance of mixing across the frontal zone by distributing nutrients to a more stable environment.

A recent study by Sokolov and Rintoul (2007) demonstrated that the ACC interacts with the bottom topography and, through upwelling, initiates algal blooms. Furthermore, nutrients (particularly iron) and Chl-a biomass are said to be advected horizontally and the system is able to retain nutrients for long periods (Sokolov and Rintoul, 2007).

The stratification of the water has been identified as one of the most important factors in limiting algal growth in oceanic regions (Llido et al., 2005). Nelson and Smith (1991) have argued that the lack of stability and mixing leads to light limitation. Llido et al. (2005) stated that strong vertical stratification occurred with a decrease in MLD. In this survey, the correlation between integrated Chl-a concentration and MLD was significant, further supporting the theory that the stratification of the water column

influences the growth of phytoplankton. Figure 15 shows the relationship between integrated Chl-a and MLD. Integrated Chl-a concentration was negatively correlated to MLD, thus when the MLD deepens, mixing increases and the Chl-a concentration decreases. The mean MLD in Subantarctic water (26.5m) was observed to be significantly shallower than in the Subtropical (58.2m) and Mixed water (46.8m) ($p<0.001$). The Subantarctic water, although nutrient rich, remains low in Chl-a concentration usually, but our survey presents results to the contrary. This may be because this specific water mass is stratified and therefore the phytoplankton are not limited by light.

A study of the trophodynamics of mesozooplankton in the region was conducted during our survey (Daly, 2008) and the mesozooplankton ingestion rates for the selected mesozooplankton species (65% of mesozooplankton abundance) ranged from 147 to 5495 ng [pig,] nd/day. Daly (2008) stated that the combined grazing impact ranged from 1.6 to 190 % of the integrated production and the highest values were recorded at the stations where the salp (*Salpa thompsoni)* and the pteropod (*Limacina retroversa)* numerically dominated the mesozooplankton counts. The mesozooplankton abundance and associated grazing are one of the controlling factors of algal population growth rate. The grazing impact in the survey region however, would have been negligible as they are not able to efficiently feed on the pico and nano-phytoplankton (Froneman, P.W., pers. comm.). The observed lack of relationship between the mesozooplankton and most of the variables (excludes negative correlation between mesozooplankton and MLD) including integrated Chl-a over the entire region further demonstrates that the mesozooplankton grazing impact was very likely to be negligible.

Martin et al. (1990) suggested that phytoplankton production is limited by the amount of iron present in the open ocean areas. The majority of iron is supplied by river run-

off along coasts and some through the mixing up of bottom sediments (Sullivan et al., 1993). The Southern Ocean is generally considered to be an area of low iron concentration. This could be the reason for the limited phytoplankton production in the region. Iron was not measured during this survey and hence one cannot gauge whether or not the survey region was iron limited.

E. Suggestions and problems concerning the study

One of the major problems of *in situ* data collection is that data collected presents a single snapshot of the region and that of the synopticity effect. It is difficult to get a good understanding of the processes occurring through the water column in the region when the processes are constantly changing as one is conducting a survey (Martin, 2005; Read et al., 2000). The grazing impacts of macrozooplankton and microzooplankton have not been assessed here and would be a future area for research. An ADCP current meter would be a good addition to future studies of this nature. The ADCP would aid in understanding the complex currents at a finer scale. I would suggest that a mooring be placed in the region. It will prove challenging to design a mooring to be placed in this tumultuous location, but it would be ideal for measuring the important variables on a constant base and throughout the water column. I would suggest iron sampling be conducted over the survey region. Additionally, a finer resolution of wind data and light intensity down the water column would have aided in some of the understanding of the processes occurring in the region.

In conclusion, phytoplankton form the basis of the marine food web and are thus of immense importance in the pelagic ecosystem of the Southern Ocean (Lutjeharms, 1985; Dower and Lucas, 1993; Laubscher et al., 1993; Weeks and Shillington, 1994). In addition, this specific region and other regions of the Southern Ocean influence the

global climate through the heat and mass exchange across the oceans and associated biologically driven carbon sink (Gille, 2002; Dower and Lucas, 1993). It is for these reasons that further investigation into understanding the dynamics in this region are highly important. In this study, the results showed how important the MLD is in determining the Chl-a concentration. Furthermore, the intense mixing in the area, associated with deeper MLDs, possibly aided by an intense weather event, hinder the ability of the phytoplankton to reproduce. This study highlights that perhaps the phytoplankton blooms during austral autumn in this region consist of smaller and shorter blooms with nano- and pico-phytoplankton dominating the region. The survey demonstrated that the location of the STC is influenced by the proximity of the ARC (Lutjeharms and Ansorge, 2001). Mixing across the STC provides an exchange of essential nutrients to the nutrient poor but well-stratified Subtropical waters thereby stimulating an increase in Chl-a concentration. The evidence suggests that the major factors in controlling Chl-a concentration at the STC are MLD and nutrient availability. These requirements are governed by the water mass mixing across the survey region.

References

Alcock, G. 2006. Does the intensification of the STC, between the southeast Atlantic and southwest Indian Oceans have an effect on primary production. *Unpublished Honours thesis*, Department of Oceanography, University of Cape Town.

Allanson, B.R., Hart, R.C. and Lutjeharms, J.R.E. 1981. Observations on the nutrients, chlorophyll and primary production of the Southern Ocean south of Africa. *South African Journal of Antarctic Research*, 10/11, 3 – 114.

Baith, K., Lindsay, R., Fu, G. and McClain, C.R. 2001. SeaDAS, a data analysis system for ocean-color satellite sensors. *EOS Trans. AGU*, 82, 202.

Barange, M., Pakamov, E.A., Perissinotto, R., Froneman, P.W., Verheye, H.M., Taunton-Clark, J. and Lucas, M.I. 1998. Pelagic community structure of the Subtropical Convergence region south of Africa and in the mid-Atlantic Ocean. *Deep-Sea Research I*, 45, 1663 - 1687.

Bartle, J.A. 1976. Euphausiids of Cook Strait: A transitional fauna? *New Zealand Journal of Marine and Freshwater Research,* 10, 559 – 576.

Bathmann, U., Priddle, J., Trguer, P., Lucas, M.I., Hall, J., Parslow, J. 2000. Plankton Ecology and Biogeochemistry in the Southern Ocean: a Review of Southern Ocean JGOFS. In: Hanson, R.B., Ducklow, H., Field, J.G. (Eds.) The Changing Ocean Carbon Cycle: A Midterm Synthesis of the Joint Global Ocean Flux Study International Geosphere – Biosphere Programme Series, 5. Cambridge University Press, Cambridge, pp. 300 – 337.

Belkin, I.M. and Gordon, A.L.1996. Southern Ocean fronts from the Greenwich meridian to Tasmania. *Journal of Geophysical Research*, 101, 3675 – 3696.

Biastoch, A. and Krauss, W. 1999. The role of mesoscale eddies in the source regions of the Agulhas Current. *Journal of Physical Oceanography*, 29, 2303 – 2317.

Blain, S., Sarthoub, G. and Laanc, P. 2008. Distribution of dissolved iron during the natural iron-fertilization experiment KEOPS (Kerguelen Plateau, Southern Ocean). *Deep-Sea Research II,* 55 (2008) 594 – 605.

Boyd, P.W., Watson, A.J., Law, C.S., Abraham, E.R., Trull, T., Murdoch, R., Bakker, C.E, Bowie, A.R., Buesseler, K.O., Chang, H., Charette, M., Croot, P., Downing, K., Frew, R., Gall, M., Hadfield, P.M., Hall, J., Harvey, M., Jameson, G., LaRoche, J., Liddicoat, M., Ling, R., Maldonado, M.T., McKay, R.M., Nodder, S., Pickmere, S., Pridmore, R., Rintoul, S., Safi, K., Sutton, P., Strzepek, R., Tanneberger, K., Turner, S., Waite, A. and Zeldis, J. 2000. A mesoscale phytoplankton bloom in the polar Southern Ocean stimulated by iron fertilization. *Nature.* 407, 695 – 702.

Boyd, P.W., Jickells, T., Law, C.S., Blain, S., Boyle, A., Buesseler, O., Coale, K.H., Cullen, J.J., de Baar, J.W., Follows, M., Harvey, M., Lancelot, C., Levasseur, M., Owens, N.P.J., Pollard, R., Rivkin, R.B., Sarmiento, J., Schoemann, V., Smetacek, V., Takeda, S., Tsuda, A., Turner, S., Watson, A.J. 2007. Mesoscale Iron Enrichment Experiments 1993–2005: Synthesis and Future Directions. *Science*, 315, 612 – 617.

Boebel, O., Rossby, T., Lutjeharms, J., Zenk, W. and Barron, C. 2003. Path and variability of the Agulhas Return Current. *Deep-Sea Research II,* 50, 35 – 56.

Buesseler, K.O., Boyd, P.W. 2003. Will ocean fertilization work? *Science*, 300 (5616) 67 - 68.

Charrette, M.A., Goneeaa, M.E., Morrisb, P.J., Stathamb, P., Fonesb, G., Planquette, H., Salterb, I., Garabatob, A.N. 2007. Radium isotopes as tracers of iron sources fueling a Southern Ocean phytoplankton bloom. *Deep-Sea Research II,* 54 (2007) 1989 – 1998

Comiso, J.C., McLain, C.R., Sullivan, C.W., Ryan, J.P., Leonard, C.L. 1993. Coastal zone scanner pigment concentration in the southern ocean and relationships to geophysical surface features. *Journal of Geophysical Research,* 98(C2), 2419 – 2451.

Daly, R. and Froneman, P.W. 2008.Trophodynamics of selected mesozooplankton in the region of the Subtropical Convergence in the Indian sector of the Southern Ocean. *Unpublished Masters thesis*, Department of Zoology and Entomology, Rhodes University.

Darbyshire, M., 1966. The surface waters near the coasts of Southern Africa. *Deep-Sea Research* 13, 57Ð81.

Deacon, G.E.R. 1937. The Hydrology of the Southern Ocean. *Discovery Report* 15.

DeBoyer Montégut, C., G. Madec, A. S. Fischer, A. Lazar, and D. Iudicone .2004. Mixed layer depth over the global ocean: An examination of profile data and a profile-based climatology, *Journal of Geophyical Research*, 109, C12003, doi:10.1029/2004JC002378.

Dower, K.M. and Lucas, M.I. 1993. Photosynthesis irradiance relationships and production associated with a warm core ring shed from the Agulhas Retroflection south of Africa. *Marine Ecology Progress Series,* 95, 141 – 154.

Fiala, M., Delille, B., Dubreuil, C., Kopczynska, E., Leblanc, K., Morvan, J., Queguiner, b., Blain, S., Cailliau, C., Conan, P., Corvaisier, R., Denis, M., Frankignouelle, M., Orilo,L. and Roy, S. 2003. Mesoscale surface distribution of biogeochemical characteristics in the Crozet Basin frontal zones (South Indian Ocean). *Marine Ecology Progress Series*, 249, 1 – 14.

Feldman, G. C., McClain C. R., Ocean Color Web, MODIS, Reprocessing 1.1, NASA Goddard Space Flight Center. Eds. Kuring, N., Bailey, S. W. 15 December 2008. http://oceancolor.gsfc.nasa.gov/MODISA/L3BIN/2007.

Froneman, P.W., Ansorge, I.J., Richoux, N., Blake, J., Daly, R., Sterley, J., Mostert, B., Heyns, E., Sheppard, J., Kuyper, B., Hart, N., George, C., Howard, J., Mustafa, E., Pey, Lutjeharms, J.R.E. 2007. Physical and biological processes at the Subtropical Convergence in the South-west Indian Ocean. South African Journal of Science. 103, 193 -195.

Froneman, P.W., McQuaid, C.D., Laubscher, R.K. 1999. Size-fractioned primary production studies in the vicinity of the Subtropical Front and an adjacent warm-core eddy south of Africa in austral winter. *Journal of Plankton Research,* 21, 2019 – 2035.

Froneman, P.W., McQuaid, C.D., Perissinotto, R. 1995. Biogeographic structure of microphytoplankton assemblages of the south Atlantic and Southern Ocean during austral summer. *Journal of Plankton Research*, 17, 1791 – 1802.

Frontier, S. 1977. Interface entre deux ecosytemes exemples dans le domaine pelagique. *Journal du Recerche Oceanographique*, 2, 24 – 25.

Ganachaud, A. and Wunsch, C. 2000. Improved estimates of global ocean circulation, heat transport and mixing from hydrographic data. *Nature*, 408 (6811), 453 – 457.

Gille S.T. 2002. Warming of the Southern Ocean since the 1950s. *Science. 295*, 1275 - 1277.

Gordon, A. L., Molinelli, E., Baker, T. 1978. Large-scale relative dynamic topography of Southern Ocean. *Journal of Geophysical Research Letters*, 83 NC6.

Grasshoff, K., Ehrhardt, M. and Kremling, K. 1983 Methods for seawater analysis. 2nd edition, Verlag Chemie, Weinheim, Germany.

Hara, S., Tanoue, E. 1985. Protists along 150°E in the Southern Ocean: its composition, stock and distribution. *Transactions of the Tokyo University of Fisheries,* 6, 99 - 115.

Holliday, N.P. and Read, J.F. 1998. Surface ocean fronts between Africa and Antarctica. *Deep Sea Research I*, 45, 217 - 238

Howarth, R.W. 1988. Nutrient limitation of net primary production in marine ecosystems. *Annual Review of Ecology,* 19, 89 -110.

Iocudine, D., Speich, S., Madec, G. and Blanke, B. 2008. The Global Conveyor Belt from a Southern Ocean Perspective. *Journal of Physical Oceanography,* 38, 1401 – 1425.

Joyce, T.M., Patterson, S.L., and Millard Jr., R.C., 1981. Anatomy of a cyclonic ring in the Drake Passage. *Deep-Sea Research 28A*, 1265 –1287.

Laubscher, R.K., Perissinotto, R. and McQuaid, C.D. 1993. Phytoplankton production and biomass at frontal zones in the Atlantic sector of the Southern Ocean. *Polar Biology. 13*, 471- 481.

Llido, J. Garcon, V., Lutjeharms, J.R.E. and Sudre, I. 2005. Event-scale blooms drive enhanced primary production at the Subtropical Convergence. *Geophysical Research Letters,* 32, L15611.

Longhurst, A. 1998. Ecological Geography of the Sea. Elsevier, New York.

Lutjeharms, J.R.E. and Valentine, H.R. 1984. Southern Ocean thermal fronts south of Africa. *Deep-Sea Research*, 31, 1461 – 1476.

Lutheharms, J.R.E. 1985. Location of frontal zones between Africa and Antarctica: some preliminary results. *Deep Sea Research*, 32, 1499 – 1509.

Lutjeharms, J.R.E. 1988a. Examples of extreme circulation events of the Agulhas Retroflection. *South African Journal of Science*, 84, 584 – 586.

Lutjeharns, J.R.E. 1988b. Meridional heat transport across the Subtropical Convergence by a warm eddy. *Nature*, 331, 251 – 253.

Lutjeharms, J.R.E., Valentine, H.R. and Ballegooyen, R.C. 1993. On the Subtropical Convergence in the South Atlantic Ocean. *South African Journal of Science,* 89, 552 – 559.

Lutjeharms, J.R.E. and Ansorge, I.J. 2001. The structure and transport of the Agulhas Return Current between South Africa and 70°E. *Journal of Marine Systems*, 30, 115 – 1138.

Lutjeharms, J.R.E. 2007. Three decades of research on the greater Agulhas Current. *Ocean Science*, 3, 129 – 147.

Margalef, R. 1978. Life-forms of phytoplankton as survival alternatives in an unstable environment. *Oceanologica Acta* 1(4) 493 – 509.

Martin, J.H., Fitzwater, S.E., Gordon, R.M. 1990. Iron deficiency limits algal growth in Antarctic waters. *Global Biogeochemical Cycles,* 4, 5 – 12.

Martin, A.P., Zubkov, M.V., Burkill, P.H. and Holland, R.J. 2005. Extreme spatial variability in marine picoplankton and its consequences for interpretation of Eulerian time-series. *Biology Letters,* 1 (3), 366 – 369.

McCartney, M.S., Talley, L.D. 1982. The Sub-polar mode water of the North-Atlantic Ocean. *Journal of Physical Oceanography*, 12 (11), 1169 – 1188.

Metzl, N., Tilbrook, B and Poisson, A.1999. The annual fCO_2 cycle and the air-sea CO_2 flux in the Subantarctic Ocean. *Tellus,* 51, 849 – 1861.

Morrow, R., Donguy, J-R., Chaigneau, A., and Rintoul, S.R. 2004. Cold-core anomalies at the Subantarctic front, south of Tasmania. *Journal of Marine Systems.* 51 (11), 1417 – 1440.

Nelson, D.M., Smith Jr, W.O. 1991. Sverdrup re-visited: critical depths, maximum chlorophyll levels, and the control of Southern Ocean productivity by the irradiance-mixing regime. *Limnology and Oceanography,* 36, 1650 – 1661.

Nowlin, W.D. and Klinck, J.M. 1986. The physics of the Antarctic Circumpolar Current. *Reviews of Geophysics*, 24 (3), 469 – 491.

Oschlies, A. and Garcon, V. 1998. Eddy-induced enhancement of primary production in a model of the North Atlantic Ocean. *Nature*, 394, 266 – 269.

Pakamov, E.A., McQuaid, C.D. 1996. Distribution of surface zooplankton and seabirds across the Southern Ocean. *Polar Biology*,16, 271 – 286.

Petersen, R.G. and Stramma, L. 1991. Upper-level circulation in the Southern Atlantic Ocean. *Progress in Oceanography,* 26, 1 – 73.

Pollard, R.T.,Salter, I., Sanders, R.J., Lucas, M.I., Moore, C.M., Mills, R.A., Statham, P.J., Allen, J.T., Baker, A.R., Bakker, D.C., Charette, M.A., Fielding, S., Fones, G.R., French, M., Hickma, A.E., Holland, R.J., Hughes, J.A., Jickells, T.D., Lampitt, R.S., Morris, P.J., Nedelec, F.H., Nielsdottir, M., Planquette, H., Popova, E.E., Poulton, A.J., Read, J.F., Seeyave, S., Smith, T., Stinchcombe, M., Taylor, S., Thomalla, S., Venebales, H.J., Williamson, R., Zubkov, V. 2009. Southern Ocean deep-water carbon export enhanced by natural iron fertilization. *Nature,* 457 doi:10.1038/nature07716.

Quikscat http://manati.orbit.nesdis.noaa.gov/quikscat/ Accessed 19th December 2008.

Read, J.F., Lucas, M.I., Holley, S.E. and Pollard, R.T. 2000. Phytoplankton, nutrients and hydrography in the frontal zone between the Southwest Indian Subtropical gyre and the Southern Ocean. *Deep Sea Research, Part II*, 49, 1823 – 1842.

Read, J.F. and Pollard, R.T. 1993. Structure and transport of the Antarctic Circumpolar Current and the Agulhas Return Current at 40°E. *Journal of Geophysical Research*, 98, 12281 – 12295.

Roberts, P.E. 1980. Surface distribution of albacore tuna, Thunnus alalunga Bonaterre, in relation to the Subtropical Convergence Zone east of New Zealand. New Zealand *Journal of Marine and Freshwater Research*, 14, 373 – 380.

Roden, G. I. 1975. On North Pacific temperature, salinity, sound velocity and density fronts and their relation to the wind and energy flux fields, *Journal of Physical. Oceanography*, 5, 557 – 571.

Schlitzer, R., Ocean Data View, http://odv.awi-bremerhaven.de, 2004.

Smythe-Wright, D., Chapman, P., Duncombe Rae, C., Shannon, L.V. and Boswell, S.M. 1998. Characteristics of thee South Atlantic Subtropical Frontal Zone between 15°W and 5°E. *Deep Sea Research I*, 45, 162 – 1192.

Sokolov, S. and Rintoul, S.R. 2007. On the relationship between fronts of the Antarctic Circumpolar Current and surface chlorophyll concentrations in the Southern

Ocean. *Journal of Geophysical Research* 112, C070390, doi:10.1029/2006JC004072.

Sommer, U. 1994a. The impact of light intensity and day length on silicate and nitrate competition among marine phytoplankton. *Limnology and Oceanography,* 39 (7), 1680 – 1688.

Sommer, U. 1994b. Are marine diatoms favoured by high Si:N ratios? *Marine Ecology Progress Series,* 115, 309 – 315.

StatSoft, Inc. (2002). *STATISTICA* for Windows [Computer program manual]. Tulsa, OK.

Sullivan, C.W., Arrigo, K.R., McClain, C.R., Comiso, J.R. and Firestone, J. 1993. Distribution of phytoplankton blooms in the Southern Ocean. *Science,* 262, 1832 – 1837.

Trenberth K. E., Large, W.G. and Olson, J.G. 1990. The mean annual cycle in global ocean wind stress. *Journal of Physical Oceanography,* 30,1742 - 1760.

Weeks, S.J. and Shillington, F.A. 1996. Phytoplankton pigment distribution and frontal structure in the subtropical convergence region south of Africa. *Deep-Sea Research I*, 43: 739 – 768.

Zubova, E. Ju., Timofeev, S.F.1989. Zooplankton of frontal zones and fractal geometry. *Proceedings IV All-Union Conference*, Sebastopol, pp. 70.

Appendices

Appendix 1: Matrix showing the correlation values (r-values) and significance levels (p-values) of the variables measured across the region.

Correlations (Integrated_Nutrients) Marked correlations are significant at p < .05000 N=45 (Casewise deletion of missing data)

	Phosphates (uM)	Nitrates (uM)	Silicates (uM)	Oxygen (ml/L)	Integrated Chl-a (mg chl-a.m^{-2})	Mixed Layer Depth (DeBoyer Definition)	Transformed Mesozooplankton (Root Root)	Temperature at 10m (Surface)
Phosphates (uM)	1.0000	.8779	.3463	.5589	.5122	-.5899	.0001	-.7647
	p= ---	**p=.000**	**p=.020**	**p=.000**	**p=.000**	**p=.000**	p=1.00	**p=.000**
Nitrates (uM)	.8779	1.0000	.1514	.6568	.4511	-.4584	-.0508	-.8819
	p=.000	p= ---	p=.321	**p=.000**	**p=.002**	**p=.002**	p=.740	**p=.000**
Silicates (uM)	.3463	.1514	1.0000	-.2275	-.0014	-.0851	.0794	.0692
	p=.020	p=.321	p= ---	p=.133	p=.993	p=.578	p=.604	p=.652
Oxygen (ml/L)	.5589	.6568	-.2275	1.0000	.3374	-.3605	-.1238	-.6118
	p=.000	**p=.000**	p=.133	p= ---	**p=.023**	**p=.015**	p=.418	**p=.000**
Integrated Chl-a (mg chl-a.m^{-2})	.5122	.4511	-.0014	.3374	1.0000	-.3741	.1636	-.5861
	p=.000	**p=.002**	p=.993	**p=.023**	p= ---	**p=.011**	p=.283	**p=.000**
Mixed Layer Depth (DeBoyer Definition)	-.5899	-.4584	-.0851	-.3605	-.3741	1.0000	-.2950	.5325
	p=.000	**p=.002**	p=.578	**p=.015**	**p=.011**	p= ---	**p=.049**	**p=.000**
Transformed Mesozooplankton (Root Root)	.0001	-.0508	.0794	-.1238	.1636	-.2950	1.0000	-.0547
	p=1.00	p=.740	p=.604	p=.418	p=.283	**p=.049**	p= ---	p=.721
Temperature at 10m (Surface)	-.7647	-.8819	.0692	-.6118	-.5861	.5325	-.0547	1.0000
	p=.000	**p=.000**	p=.652	**p=.000**	**p=.000**	**p=.000**	p=.721	p= ---

Appendix 2 Levene's test for homogeneity of variances for the variables across all groups

Levene Test of Homogeneity of Variances (Integrated_Nutrients) Marked effects are significant at p < .05000

	SS - Effect	df - Effect	MS - Effect	SS - Error	df - Error	MS - Error	F	p
Phosphates (uM)	0.0333	2	0.0166	0.852	42	0.0203	0.81994	0.447385
Nitrates (uM)	58.8348	2	29.4174	69.959	42	1.6657	17.66077	0.000003
Silicates (uM)	0.4451	2	0.2225	45.902	42	1.0929	0.20362	0.816570
Oxygen (ml/L)	0.0664	2	0.0332	4.869	42	0.1159	0.28633	0.752467
Integrated Chl-a (mg chl-a.m$^{-2)}$	111.3811	2	55.6905	638.403	42	15.2001	3.66383	0.034146
Mixed Layer Depth (DeBoyer Definition)	642.0913	2	321.0457	5699.449	42	135.7012	2.36583	0.106267
Transformed Mesozooplankton (Root Root)	3.7718	2	1.8859	191.438	42	4.5580	0.41376	0.663828

Appendix 3(a) Matrix showing the ANOVA test for differences between water mass groups' means (univariate)

Analysis of Variance (Integrated_Nutrients) Marked effects are significant at p < .05000

	SS - Effect	df - Effect	MS - Effect	SS - Error	df - Error	MS - Error	F	p
Phosphates (uM)	2.403	2	1.202	2.18	42	0.0518	23.17970	0.000000
Nitrates (uM)	723.311	2	361.656	277.05	42	6.5965	54.82510	0.000000
Silicates (uM)	1.716	2	0.858	88.36	42	2.1039	0.40770	0.667782
Oxygen (ml/L)	10.169	2	5.084	12.56	42	0.2991	16.99791	0.000004
Integrated Chl-a (mg chl-a.m$^{-2)}$	834.390	2	417.195	1760.81	42	41.9241	9.95121	0.000290
Mixed Layer Depth (DeBoyer Definition)	6954.181	2	3477.090	17737.31	42	422.3170	8.23337	0.000962
Transformed Mesozooplankton (Root Root)	7.344	2	3.672	521.12	42	12.4076	0.29595	0.745365

Appendix 3(b) Matrix showing the ANOVA test for differences between water mass groups' means (multivariate)

Multivariate Tests of Significance (Integrated_Nutrients.sta) Sigma-restricted parameterization Type I decomposition

	Test	Value	F	Effect - df	Error - df	p
Intercept	Wilks	0.004071	1258.063	7	36	0.000000
Water Mass Group	Wilks	0.169067	7.365	14	72	0.000000

Appendix 4 (a-g) Tables showing the results of the Tukey HSD test of significant difference between water mass groups' variable means

(a) Phosphates

Tukey HSD test; variable **Phosphates** (uM) Approximate Probabilities for Post Hoc Tests Error: Between MS = .05184, df = 42.000

Water Mass Group	{1} - 1.1094	{2} - .67630	{3} - .53797
1 Sub-Antarctic		0.000130	0.000119
2 Mixed	0.000130		0.215319
3 Sub-tropical	0.000119	0.215319	

(b) Oxygen

Tukey HSD test; variable Oxygen (ml/L) Approximate Probabilities for Post Hoc Tests Error: Between MS = .29912, df = 42.000

Water Mass Group	{1} - 6.4580	{2} - 5.5390	{3} - 5.2972
1 Sub-Antarctic		0.000214	0.000123
2 Mixed	0.000214		0.436530
3 Sub-tropical	0.000123	0.436530	

(c) Integrated Chl-a

Tukey HSD test; variable Integrated Chl-a (mg chl-a.m-2) Approximate Probabilities for Post Hoc Tests Error: Between MS = 41.924, df = 42.000

Water Mass Group	{1} - 26.532	{2} - 21.939	{3} - 15.499
1 Sub-Antarctic		0.137884	0.000300
2 Mixed	0.137884		0.021142
3 Sub-tropical	0.000300	0.021142	

(d) Mixed Layer Depth

Tukey HSD test; variable **Mixed Layer Depth** (DeBoyer Definition) Approximate Probabilities for Post Hoc Tests Error: Between MS = 422.32, df = 42.000

	Water Mass Group	{1} - 26.478	{2} - 46.886	{3} - 58.204
1	Sub-Antarctic		0.024709	0.000812
2	Mixed	0.024709		0.280501
3	Sub-tropical	0.000812	0.280501	

(e) Transformed Mesozooplankton

Tukey HSD test; variable **Transformed Mesozooplankton** (Root Root) Approximate Probabilities for Post Hoc Tests Error: Between MS = 12.408, df = 42.00

	Water Mass Group	{1} - 13.258	{2} - 13.686	{3} - 12.721
1	Sub-Antarctic		0.940433	0.917499
2	Mixed	0.940433		0.723763
3	Sub-tropical	0.917499	0.723763	

(f) Silicates

Tukey HSD test; variable Silicates (uM) Approximate Probabilities for Post Hoc Tests Error: Between MS = 2.1039, df = 42.000

	Water Mass Group	{1} - 4.6335	{2} - 5.0836	{3} - 4.7559
1	Sub-Antarctic		0.672831	0.973973
2	Mixed	0.672831		0.802399
3	Sub-tropical	0.973973	0.802399	

(g) Nitrates

Tukey HSD test; variable Nitrates (uM) Approximate Probabilities for Post Hoc Tests Error: Between MS = 6.5965, df = 42.000

	Water Mass Group	{1} - 11.362	{2} - 3.7869	{3} - 1.4782
1	Sub-Antarctic		0.000119	0.000119
2	Mixed	0.000119		0.040435
3	Sub-tropical	0.000119	0.040435	

Appendix 5 a, b & c Matrix showing the correlation values (r-values) and significance levels (p-values) of the variables measured at the Sub-Antarctic, Mixed and Subtropical water masses.

(a) Sub-Antarctic water mass correlation matrix

Water Mass Group=Sub-Antarctic Correlations Marked correlations are significant at p < .05000 N=13 (Casewise deletion of missing data)

	Phosphates (uM)	Nitrates (uM)	Silicates (uM)	Oxygen (ml/L)	Integrated Chl-a (mg chl-a.m$^{-2)}$	Mixed Layer Depth (DeBoyer Definition)	Transformed Mesozooplankton (Root Root)
Phosphates (uM)	1.0000	.8434	.6298	.4892	.4159	.3110	-.3766
	p= ---	**p=.000**	**p=.021**	p=.090	p=.158	P=.301	p=.205
Nitrates (uM)	.8434	1.0000	.6713	.5054	.2689	.4038	-.6563
	p=.000	p= ---	**p=.012**	p=.078	p=.374	P=.171	**p=.015**
Silicates (uM)	.6298	.6713	1.0000	.0388	-.1895	.5276	-.5885
	p=.021	**p=.012**	p= ---	p=.900	p=.535	P=.064	**p=.034**
Oxygen (ml/L)	.4892	.5054	.0388	1.0000	.2955	-.0654	.0056
	p=.090	p=.078	p=.900	p= ---	p=.327	P=.832	p=.985
Integrated Chl-a (mg chl-a.m$^{-2)}$	.4159	.2689	-.1895	.2955	1.0000	.0907	-.0248
	p=.158	p=.374	p=.535	p=.327	p= ---	P=.768	p=.936
Mixed Layer Depth (DeBoyer Definition)	.3110	.4038	.5276	-.0654	.0907	1.0000	-.5695
	p=.301	p=.171	p=.064	p=.832	p=.768	P= ---	p=.042
Transformed Mesozooplankton (Root Root)	-.3766	-.6563	-.5885	.0056	-.0248	-.5695	1.0000
	p=.205	**p=.015**	**p=.034**	p=.985	p=.936	**P=.042**	p= ---

(b) Mixed water mass correlation matrix

Water Mass Group=Mixed Correlations (Integrated_Nutrients.sta) Marked correlations are significant at p < .05000 N=18 (Casewise deletion of missing data)

	Phosphates (uM)	Nitrates (uM)	Silicates (uM)	Oxygen (ml/L)	Integrated Chl-a (mg chl-a.m^{-2})	Mixed Layer Depth (DeBoyer Definition)	Transformed Mesozooplankton (Root Root)
Phosphates (uM)	1.0000	.7644	.5901	-.0032	.1101	-.6847	.2065
	p= ---	**p=.000**	**P=.010**	p=.990	p=.664	**p=.002**	p=.411
Nitrates (uM)	.7644	1.0000	.2559	.0687	-.2723	-.3712	.1325
	p=.000	p= ---	P=.305	p=.787	p=.274	p=.129	p=.600
Silicates (uM)	.5901	.2559	1.0000	-.3459	.1177	-.2160	.4293
	p=.010	p=.305	P= ---	p=.160	p=.642	p=.389	p=.075
Oxygen (ml/L)	-.0032	.0687	-.3459	1.0000	-.2781	-.1828	-.3071
	p=.990	p=.787	P=.160	p= ---	p=.264	p=.468	p=.215
Integrated Chl-a (mg chl-a.m^{-2})	.1101	-.2723	.1177	-.2781	1.0000	-.3004	.3143
	p=.664	p=.274	P=.642	p=.264	p= ---	p=.226	p=.204
Mixed Layer Depth (DeBoyer Definition)	-.6847	-.3712	-.2160	-.1828	-.3004	1.0000	-.0077
	p=.002	p=.129	P=.389	p=.468	p=.226	p= ---	p=.976
Transformed Mesozooplankton (Root Root)	.2065	.1325	.4293	-.3071	.3143	-.0077	1.0000
	p=.411	p=.600	P=.075	p=.215	p=.204	p=.976	p= ---

(c) Sub-tropical water mass correlation matrix

Water Mass Group=Sub-tropical Correlations (Integrated_Nutrients.sta) Marked correlations are significant at p < .05000 N=14 (Casewise deletion of missing data)

	Phosphates (uM)	Nitrates (uM)	Silicates (uM)	Oxygen (ml/L)	Integrated Chl-a (mg chl-a.m^{-2})	Mixed Layer Depth (DeBoyer Definition)	Transformed Mesozooplankton (Root Root)
Phosphates (uM)	1.0000	.2248	.4900	-.1391	.2615	-.6304	-.0356
	p= ---	p=.440	P=.075	p=.635	p=.367	**p=.016**	p=.904
Nitrates (uM)	.2248	1.0000	-.1199	-.3650	-.2880	-.4605	.5133
	p=.440	p= ---	P=.683	p=.199	p=.318	p=.097	p=.060
Silicates (uM)	.4900	-.1199	1.0000	-.4155	.1181	-.4948	.0759
	p=.075	p=.683	P= ---	p=.140	p=.688	p=.072	p=.797
Oxygen (ml/L)	-.1391	-.3650	-.4155	1.0000	.6215	.2481	-.1514
	p=.635	p=.199	P=.140	p= ---	**p=.018**	p=.392	p=.605
Integrated Chl-a (mg chl-a.m^{-2})	.2615	-.2880	.1181	.6215	1.0000	-.0294	-.0421
	p=.367	p=.318	P=.688	**p=.018**	p= ---	p=.921	p=.886
Mixed Layer Depth (DeBoyer Definition)	-.6304	-.4605	-.4948	.2481	-.0294	1.0000	-.5224
	p=.016	p=.097	P=.072	p=.392	p=.921	p= ---	p=.055
Transformed Mesozooplankton (Root Root)	-.0356	.5133	.0759	-.1514	-.0421	-.5224	1.0000
	p=.904	p=.060	P=.797	p=.605	p=.886	p=.055	p= ---

Appendix 6 (a -f) Vertical sections of Silicate, Oxygen, Nitrate, Phosphate concentrations and temperature measured along transects 1 – 6 (map shows the location of the section).

(a) Transect 1

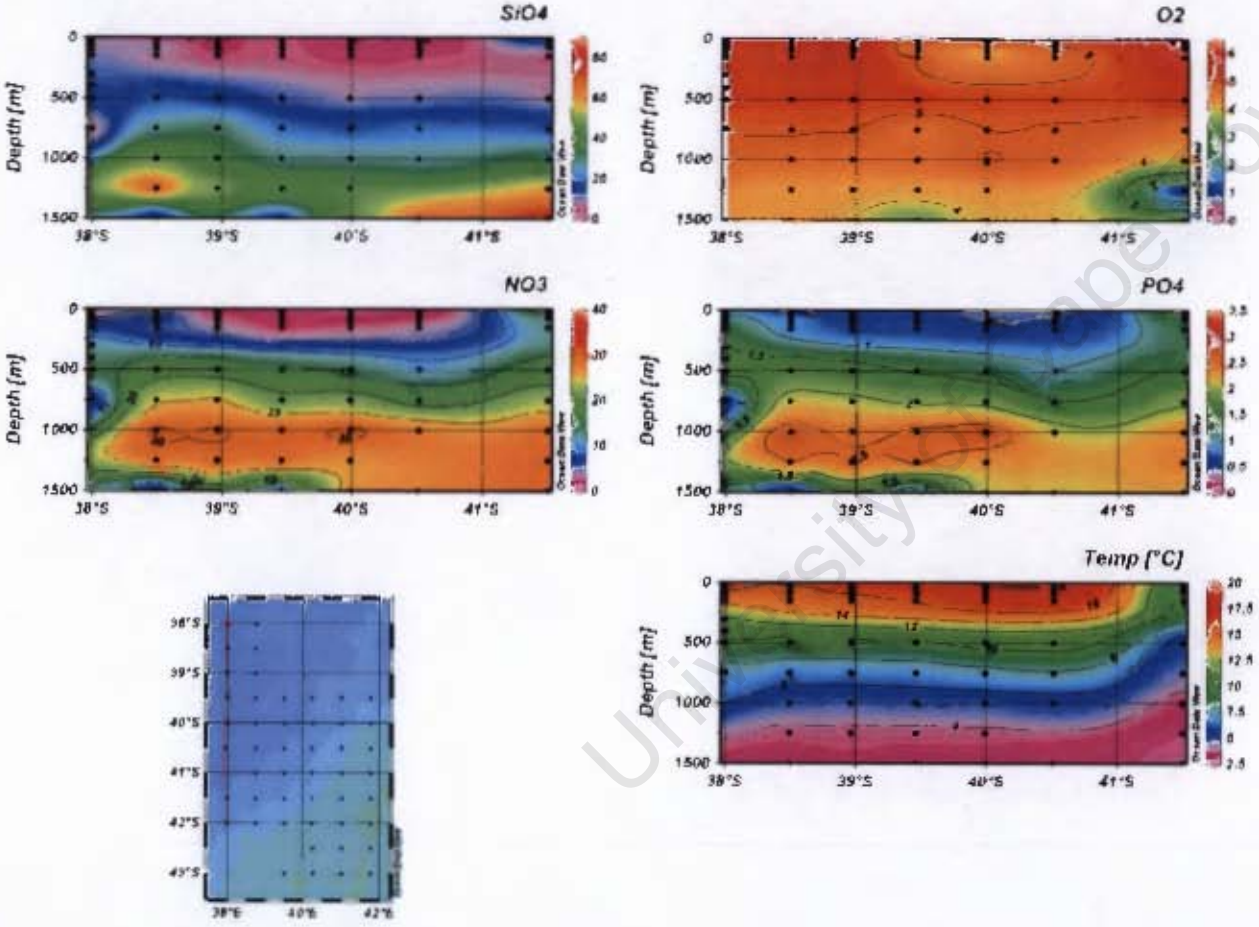

(b) Transect 2

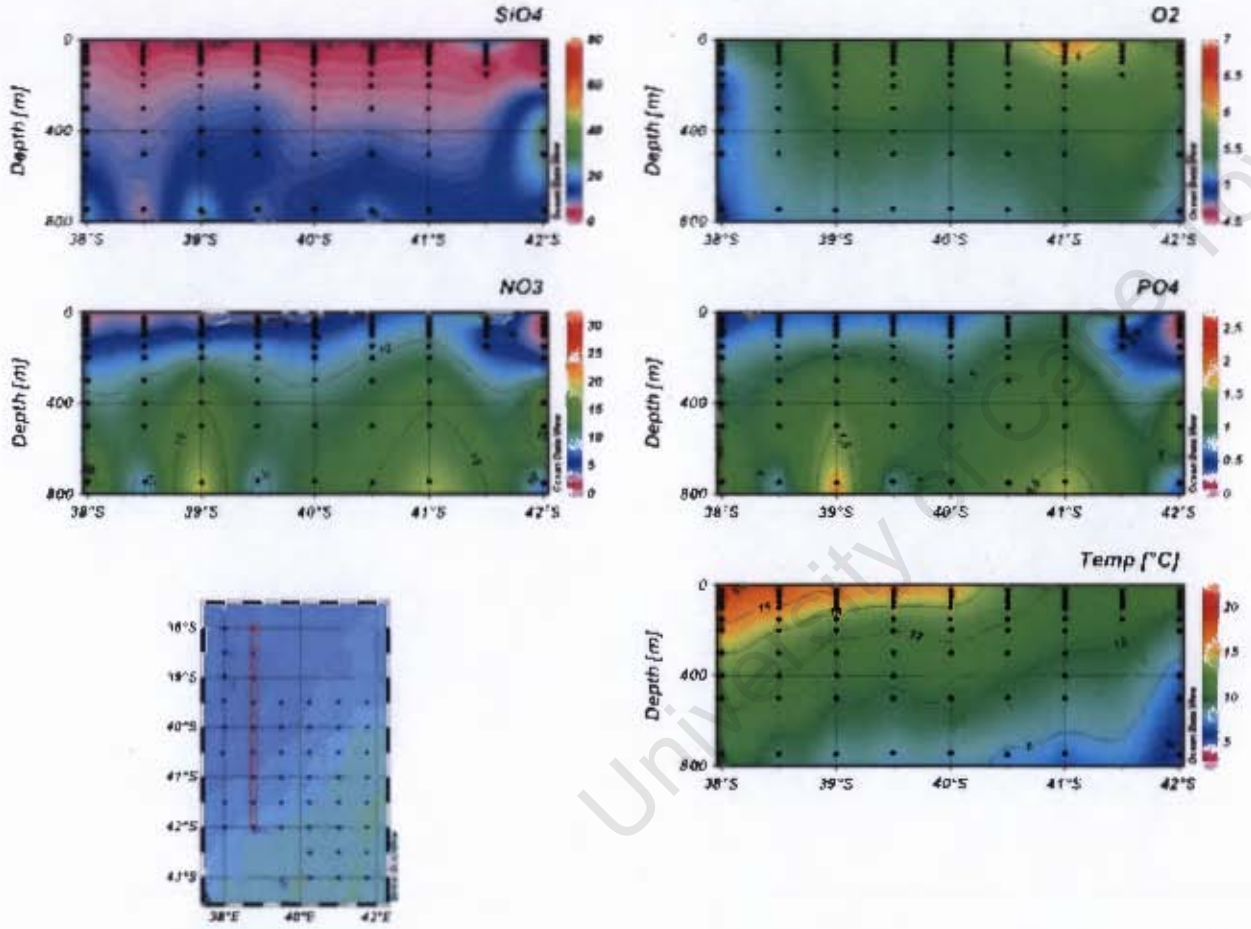

(c) Transect 3

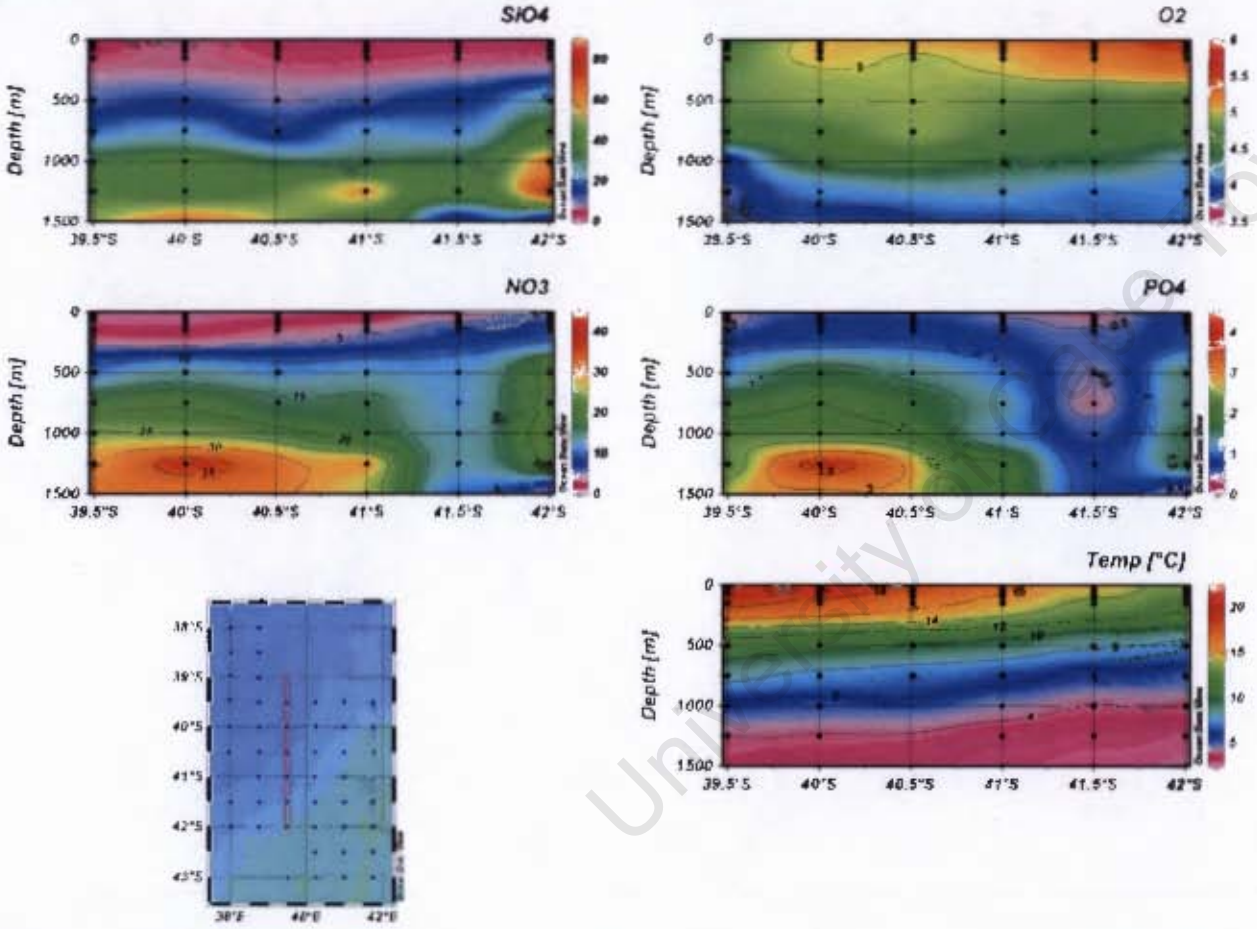

(d) Transect 4

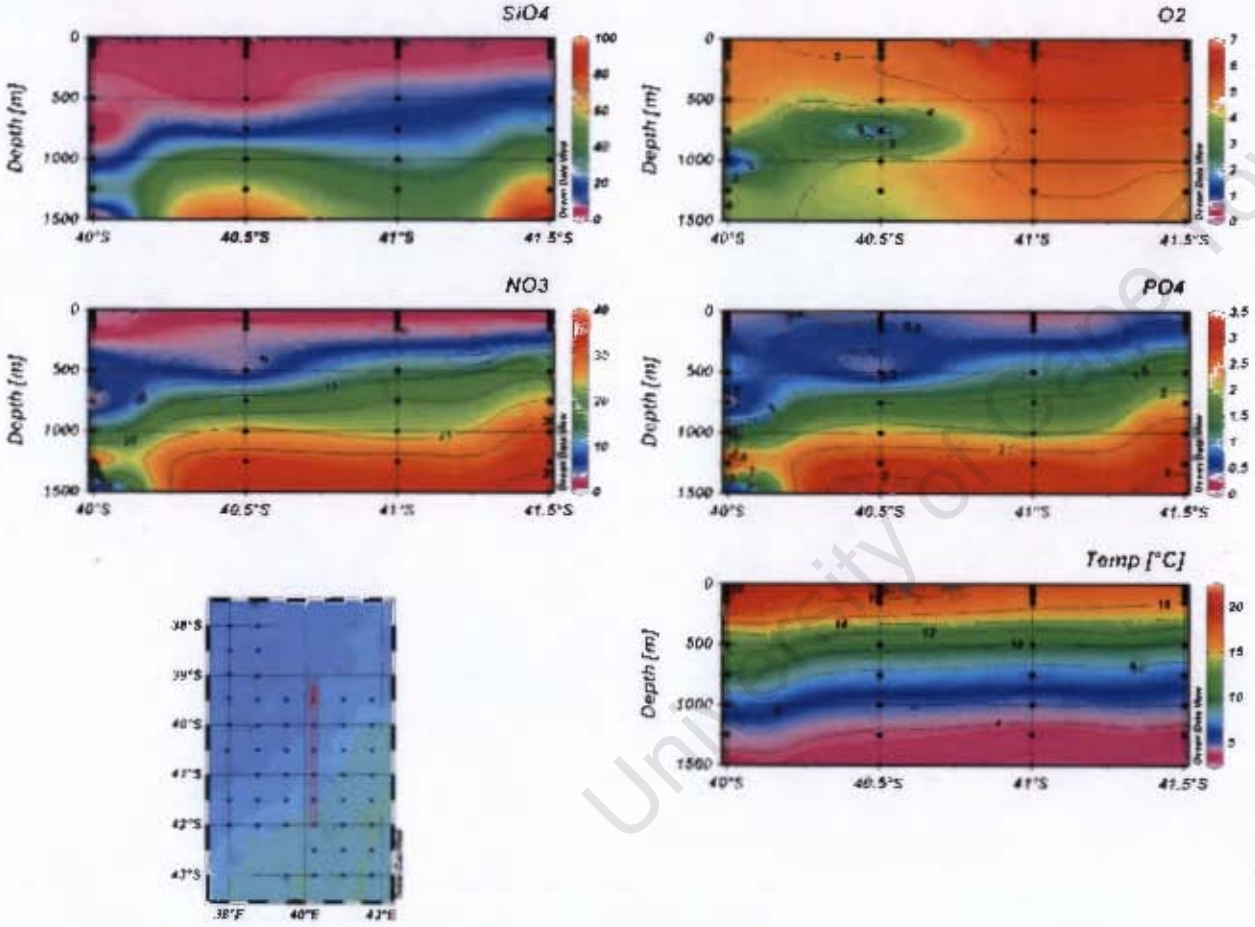

(e) Transect 5

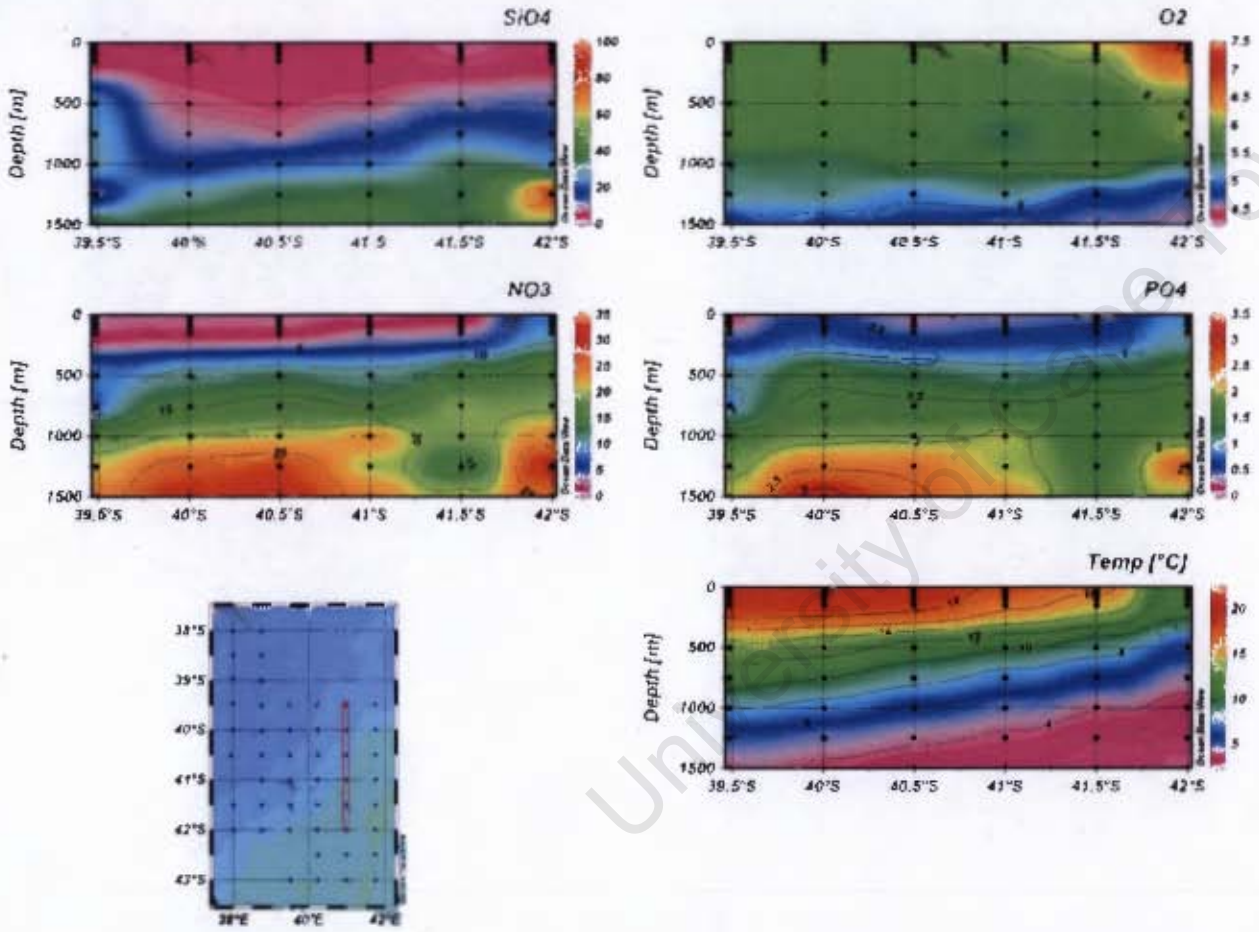

(f) Transect 6